JOURNAL OF MATHEMATICAL PHYSICS VOLUME 41, NUMBER 9 SEPTEMBER 2000

Two-dimensional, highly directive currents on large circular loops

Dionisios Margetis[a)]
Gordon McKay Laboratory, Harvard University, Cambridge, Massachusetts 02138-2901

George Fikioris
Institute of Communications and Computer Systems, Department of Electrical and Computer Engineering, National Technical University of Athens, GR 157-73 Athens, Greece

(Received 7 February 2000; accepted for publication 20 March 2000)

Properties of idealized, two-dimensional current distributions on circular loops are investigated analytically via the solution of a constrained optimization problem. The directivity in the far field is maximized under a fixed $C=N/T$, where N is the integral of the square of the current magnitude and T is the total radiated power. C enters the ensuing Fourier series for the current implicitly through a Lagrange multiplier α. For non-negative α and large electrical radius ka, the directivity and the current are evaluated approximately via combined use of the Poisson summation formula and the Mellin transform technique. As a result, a geometrical-ray representation for the current is derived for the case of directivities that are slightly larger than that of the uniform distribution. The analysis indicates certain advantages of large radiating structures for moderate values of the constraint C. In the limit $C\to\infty$ of Oseen's ''Einstein needle radiation,'' an asymptotic formula for the directivity is obtained. Possible extensions of these results to classes of smooth convex loops are briefly discussed. © *2000 American Institute of Physics.* [S0022-2488(00)04109-8]

I. INTRODUCTION

In a recent paper,[1] a theoretical scheme for studying properties of monochromatic, highly directive source distributions was formulated and analyzed. The first step is to pose a constrained optimization problem for the optimum continuous source distribution, the solution of which is then shown to satisfy a Fredholm integral equation of the second kind. In this equation, the constraint enters implicitly via a non-negative Lagrange multiplier α. In Ref. 1, the sources are classical currents along a fixed axis, generating electromagnetic fields that obey Maxwell's equations in free space.

In this paper, the aforementioned scheme is applied to two-dimensional sources that lie on large circular loops of radius a, under the condition $ka\gg 1$, where k is the wave number. These sources appear as boundary data for the scalar wave equation. Two considerations motivating this work are the following. The first consideration is that, due to the continuous rotational symmetry of the source region, the integral equation can be solved exactly. Alternatively, the optimization problem can be solved directly, with no recourse to the integral equation. Exact solutions of this type have been given elsewhere (see, e.g., Ref. 1 and the references therein, especially the studies by Katsenelenbaum and Shalukhin[2] and by Angell and co-workers[3]). The most familiar exact solution involves source distributions of uniform magnitude that generate the maximum directivity by constructive interference, herein called ''the reference case''; it corresponds to $\alpha=0$.[1] The present paper focuses on the case of large ka and positive α, where the optimum sources produce directivities higher than that of the reference case. Insight into this demanding problem is obtained

a)Electronic mail: dmarget@fas.harvard.edu

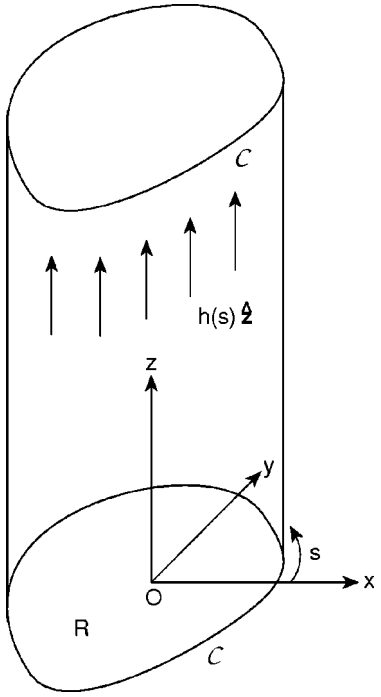

FIG. 1. The three-dimensional geometry of the problem considered in this paper (general formulation). $\mathcal{C}$ is the cross section of an infinitely long cylindrical shell that extends along the z axis. The arrows show the direction of the z-invariant surface current $h(s)\hat{\mathbf{z}}$.

by deriving simple asymptotic formulas for the optimum source distributions, as well as for the directivity. Necessarily, these sources are oscillatory in nature.

The second consideration is that, for the case of the electromagnetic fields, the source distributions may serve as a model for axially (z-) invariant surface currents flowing in infinitely long, highly conducting cylindrical shells along the axial (z) direction. The constraining quantity measures the efficiency of the radiating system in the plane transverse to the cylindrical axis.[1] The geometry is depicted in Fig. 1 for an arbitrary, simple closed curve $\mathcal{C}$ as the boundary. Notably, interesting properties of electrically large, convex cylindrical shells have been indicated by recent experimental and theoretical work on resonant circular arrays of cylindrical dipoles.[4,5] As discussed in Sec. IX, it is hoped that, conversely, the present study may offer some insight into similar properties of currents in convex, *noncircular* arrays of dipoles. Such properties have not as yet been observed experimentally. An outline of the present paper is provided in the following.

Section II is devoted to the derivation of suitable series expansions describing the optimum current, directivity, and constraint. The starting point is a familiar boundary-value problem for the wave equation in two space dimensions. In Sec. III, the reference case ($\alpha=0$) is studied in detail for a large circular loop; in particular, an asymptotic expansion is derived for the directivity. Sections IV–VI deal with the asymptotic evaluation of the directivity as a function of the constraint when $ka\gg 1$ and $\alpha>0$. In Sec. VII, the results of these calculations are discussed, with emphasis on the possible theoretical advantages of large radiating structures. Section VIII provides a description for the asymptotic behavior of the optimum current for moderate values of the constraint C. The $e^{-i\omega t}$ time dependence is suppressed throughout the analysis.

II. PRELIMINARIES

As depicted in Fig. 2, $\mathcal{C}$ is the boundary of a simply connected region R in two space dimensions, with $R\cap\mathcal{C}=\varnothing$. Consider the boundary-value problem[6]

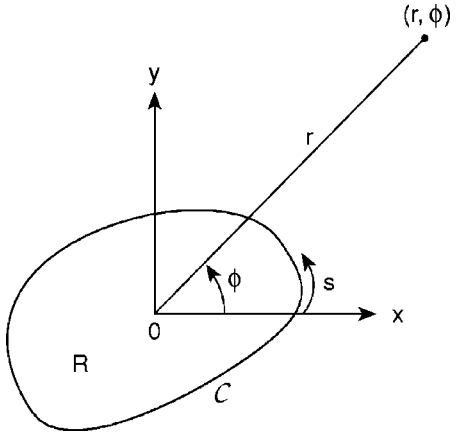

FIG. 2. The geometry of the problem in two space dimensions (general formulation). R is the cross section of the cylinder of Fig. 1 and $\mathcal{C}$ is the boundary of R.

$$\begin{aligned}
&\nabla^2 U(\mathbf{r}) + k^2 U(\mathbf{r}) = 0, && \mathbf{r} \in \mathcal{E}_2 \setminus \mathcal{C}, \\
&U(\mathbf{r}) \text{ twice continuously differentiable in } \mathcal{E}_2 \setminus \mathcal{C}, && \\
&U(\mathbf{r}) \text{ continuous across } \mathcal{C}, && \\
&\partial U^+(\mathbf{r})/\partial \eta - \partial U^-(\mathbf{r})/\partial \eta = h(s), && \mathbf{r} \in \mathcal{C}, \\
&\partial U(\mathbf{r})/\partial r - ikU(\mathbf{r}) = o(r^{-1/2}), && r = |\mathbf{r}| \to \infty,
\end{aligned} \tag{2.1}$$

where $\mathcal{E}_2$ denotes the entire two-dimensional Euclidean space, k is a fixed positive number, and $\partial U^{\pm}/\partial \eta$ is the derivative of $U(\mathbf{r})$ in the outward local normal to $\mathcal{C}$ as the position vector $\mathbf{r}$ approaches $\mathcal{C}$ from the exterior of $\mathcal{C}$ $(+)$ or from R $(-)$.[7] $h(s)$ is assumed to be continuous and have the finite norm $\sqrt{N}$, where[1]

$$N = \frac{1}{L_{\mathcal{C}}} \int_{\mathcal{C}} ds\, |h(s)|^2. \tag{2.2}$$

$L_{\mathcal{C}} = \int_{\mathcal{C}} ds$ and ds is the usual measure on $\mathcal{C}$. $U(x,y)$ is interpreted as the sole (z) component of the vector potential in the Lorentz gauge due to the surface current distribution $h(s)\hat{\mathbf{z}}$ oscillating with frequency $\omega = kc$ in a long cylindrical shell of cross section $\mathcal{C}$ (see Fig. 1), where c is the velocity of light in vacuum.

This boundary-value problem admits the solution

$$U(\mathbf{r}) = \frac{i}{4} \int_{\mathcal{C}} ds'\, H_0^{(1)}(k|\mathbf{r} - \mathbf{r}(s')|) h(s'). \tag{2.3}$$

The associated far-field pattern is defined as

$$\psi(\hat{\mathbf{r}}) = \frac{4}{L_{\mathcal{C}}} \lim_{kr \to \infty} \left[e^{-i(kr + \pi/4)} \sqrt{\frac{\pi kr}{2}} U(\mathbf{r}) \right] = \frac{1}{L_{\mathcal{C}}} \int_{\mathcal{C}} ds'\, e^{-ik\hat{\mathbf{r}}(\phi) \cdot \mathbf{r}(s')} h(s'), \tag{2.4}$$

where $\hat{\mathbf{r}} = \hat{\mathbf{r}}(\phi) = (\cos\phi, \sin\phi)$ $(0 \leqslant \phi < 2\pi)$. The power flux and the total radiated power (per unit length) are

$$S(\phi) = |\psi(\hat{\mathbf{r}})|^2, \tag{2.5}$$

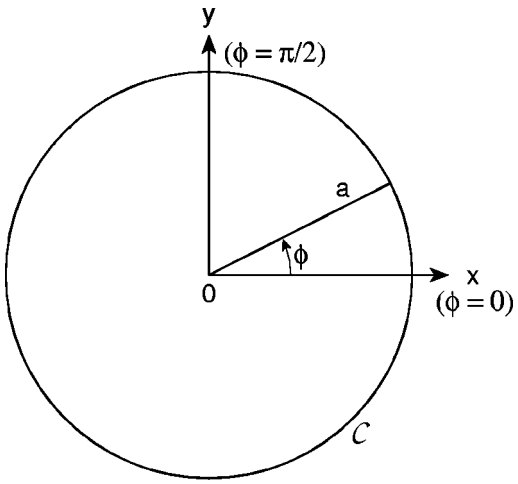

FIG. 3. The circular loop.

.

$$T=\frac{1}{2\pi}\int_0^{2\pi} d\phi\, S(\phi). \tag{2.6}$$

Following the analysis in Ref. 1, define

$$D=P/T, \quad P=S(\phi_0), \tag{2.7}$$

$$C=N/T, \tag{2.8}$$

where D is the directivity in a given direction ϕ_0. In the electromagnetic case, C measures the efficiency of the radiating system, because N is proportional to the dissipation losses.

Attention now focuses on currents that produce the maximum D under a fixed C. Such an optimum current $h(s)=\tilde{h}(s)$ uniquely solves the following problem:

Problem 2.1: Given k and $\mathcal{C}$, maximize P for fixed N, T, and phase $\mathrm{Arg}\,\psi(\hat{\mathbf{r}}_0)=0$ $[\hat{\mathbf{r}}_0=\hat{\mathbf{r}}(\phi_0)]$.

All optimum currents can be obtained via multiplication of $\tilde{h}(s)$ by arbitrary nonzero constants. By use of the method of Lagrange, $\tilde{h}(s)$ is found to satisfy a Fredholm integral equation of the second kind:[1,8]

$$\tilde{h}(s)+\frac{\alpha}{L_{\mathcal{C}}}\int_{\mathcal{C}} ds'\, J_0(k|\mathbf{r}(s)-\mathbf{r}(s')|)\tilde{h}(s')=e^{ik\hat{\mathbf{r}}(\phi_0)\cdot\mathbf{r}(s)}, \tag{2.9}$$

where α is essentially a Lagrange multiplier, taken to be non-negative, and J_n is the Bessel function of order n.

A. Optimum source distribution on the circle

When $\mathcal{C}$ is a circle of radius a centered at the origin ($s=a\phi$, as depicted in Fig. 3), $\tilde{h}(s)$ can be obtained in simple closed form. The starting point is the Fourier expansion

$$\tilde{h}(s(\phi))=j(\phi)=\sum_{n=-\infty}^{\infty} f_n e^{in\phi}, \tag{2.10}$$

where f_n are coefficients yet to be determined. It follows that

$$\psi(\hat{\mathbf{r}}) = \sum_{n=-\infty}^{\infty} f_n J_n(ka) e^{in(\phi - \pi/2)}, \tag{2.11}$$

$$P = \left| \sum_{n=-\infty}^{\infty} f_n J_n(ka) e^{in(\phi_0 - \pi/2)} \right|^2, \tag{2.12}$$

$$N = \sum_{n=-\infty}^{\infty} |f_n|^2, \tag{2.13}$$

$$T = \sum_{n=-\infty}^{\infty} |f_n|^2 J_n(ka)^2. \tag{2.14}$$

Due to the continuous rotational symmetry of the current-carrying region, it is immaterial what the value of ϕ_0 is. For definiteness, take $\phi_0 = \pi/2$. Because N and T depend only on the magnitudes $|f_n|$, it is advantageous to maximize P first by keeping all $|f_n|$ fixed and varying the phases $\mathrm{Arg}\, f_n$. For nonzero coefficient f_0, the choice

$$f_0 \ \text{real} \tag{2.15}$$

is made conveniently without loss of generality. The sign of f_0 has no significance; if f_0 is zero, a remedy is to change ka slightly by invoking the continuity of each f_n in ka. Accordingly, the maximum of

$$P = \left| \sum_{n=-\infty}^{\infty} f_n J_n(ka) \right|^2 \tag{2.16}$$

is attained by taking all f_n to be real. Consider

$$f_n J_n(ka) \geqslant 0, \quad n = 0, \pm 1, \pm 2, \ldots . \tag{2.17}$$

The task is thus assigned to maximize the function

$$\sqrt{P} = \sum_{n=-\infty}^{\infty} f_n J_n(ka), \tag{2.18}$$

by keeping fixed the N and T of Eqs. (2.13) and (2.14).

The method of Lagrange furnishes[9]

$$J_n(ka) - \lambda_1 f_n - \lambda_2 J_n(ka)^2 f_n = 0,$$

or

$$f_n = \aleph \frac{J_n(ka)}{1 + \alpha J_n(ka)^2}, \tag{2.19}$$

where $\alpha = \lambda_2/\lambda_1$, and $\aleph$ is a constant that may be set equal to 1 since it is irrelevant to the maximization of D. Consequently,

$$j(\phi;\alpha) = j(\phi) = \sum_{n=-\infty}^{\infty} \frac{J_n(ka)}{1 + \alpha J_n(ka)^2} e^{in\phi}. \tag{2.20}$$

This current generates the real far field

$$\psi(\hat{\mathbf{r}};\alpha)=\sum_{n=-\infty}^{\infty}\frac{J_n(ka)^2}{1+\alpha J_n(ka)^2}e^{in(\phi-\pi/2)}. \tag{2.21}$$

The ensuing optimum quantities of interest are

$$\sqrt{P(\alpha)}=\sum_{n=-\infty}^{\infty}\frac{J_n(ka)^2}{1+\alpha J_n(ka)^2}, \tag{2.22}$$

$$N(\alpha)=\sum_{n=-\infty}^{\infty}\frac{J_n(ka)^2}{[1+\alpha J_n(ka)^2]^2}, \tag{2.23}$$

$$T(\alpha)=\sum_{n=-\infty}^{\infty}\frac{J_n(ka)^4}{[1+\alpha J_n(ka)^2]^2}. \tag{2.24}$$

Alternatively, one may expand the kernel of the integral equation (2.9) as[10]

$$J_0(w)=\sum_{n=-\infty}^{\infty}J_n(ka)^2e^{in(\phi-\phi')},\quad w=2ka\sin\left(\frac{\phi-\phi'}{2}\right),\quad \phi,\phi'\in[0,2\pi). \tag{2.25}$$

The eigenfunctions of the homogeneous counterpart of Eq. (2.9) are $e^{in\phi}$ for the circle (n: integer), with eigenvalues $\alpha_n=-J_n(ka)^2$. The procedure to obtain Eq. (2.20) is outlined in Appendix E of Ref. 1.

B. Alternative representations

The original series representations (2.20) and (2.22)–(2.24) can be converted into series of integrals by application of the Poisson summation formula (see Appendix A).[11] Thus,

$$j(\phi)=\sum_{m=-\infty}^{\infty}\int_0^{\infty}d\nu\,\frac{J_\nu(ka)}{1+\alpha J_\nu(ka)^2}[e^{i\nu\phi}+e^{i\nu(\pi-\phi)}]e^{i2\pi m\nu}, \tag{2.26}$$

$$\sqrt{P(\alpha)}=2\sum_{m=-\infty}^{\infty}\int_0^{\infty}d\nu\,\frac{J_\nu(ka)^2}{1+\alpha J_\nu(ka)^2}e^{i2\pi m\nu}, \tag{2.27}$$

$$N(\alpha)=2\sum_{m=-\infty}^{\infty}\int_0^{\infty}d\nu\,\frac{J_\nu(ka)^2}{[1+\alpha J_\nu(ka)^2]^2}e^{i2\pi m\nu}, \tag{2.28}$$

$$T(\alpha)=2\sum_{m=-\infty}^{\infty}\int_0^{\infty}d\nu\,\frac{J_\nu(ka)^4}{[1+\alpha J_\nu(ka)^2]^2}e^{i2\pi m\nu}. \tag{2.29}$$

Introduce

$$A(\nu)=\tfrac{1}{2}H_\nu^{(1)}(ka),\quad B(\nu)=\tfrac{1}{2}H_\nu^{(2)}(ka). \tag{2.30}$$

There exist functions $\tau_1=\tau_1(\nu)$ and $\tau_2=\tau_2(\nu)$ such that

$$1+i\sqrt{\alpha}\,J_\nu(ka)=\tau_2(1+\tau_1A)(1+\tau_1B). \tag{2.31}$$

This equation leads to a system of nonlinear equations for $\tau_1(\nu)$ and $\tau_2(\nu)$, viz.,

$$\tau_2(1+\tau_1^2AB)=1,\quad \tau_1\tau_2=i\sqrt{\alpha}, \tag{2.32}$$

with the solution

$$\tau_1=\frac{2i\sqrt{\alpha}}{1+\sqrt{1+4\alpha AB}},\quad \tau_2=\frac{1}{2}(1+\sqrt{1+4\alpha AB}). \tag{2.33}$$

Successive decompositions into partial fractions give

$$\frac{J_\nu(ka)}{1+\alpha J_\nu(ka)^2}=\frac{(-2i\sqrt{\alpha})^{-1}}{1+i\sqrt{\alpha}J_\nu(ka)}-\frac{(-2i\sqrt{\alpha})^{-1}}{1-i\sqrt{\alpha}J_\nu(ka)}$$
$$=\frac{1}{\tau_2^2+\alpha AB}\left[\frac{A}{1-(\tau_1 A)^2}+\frac{B}{1-(\tau_1 B)^2}\right]. \tag{2.34}$$

In this last expression, only the bracketed terms exhibit oscillations in ν to leading order in $(ka)^{-1}$ when $ka\gg 1$. In the following, Eqs. (2.26)–(2.29) are treated analytically for $ka\gg 1$.

III. REFERENCE CASE ($\alpha=0$)

The case with $\alpha=0$ deserves some special attention. The resulting optimum current is the familiar uniform distribution

$$j(\phi;0)=\sum_{n=-\infty}^{\infty} J_n(ka)e^{in\phi}=e^{ika\sin\phi}. \tag{3.1}$$

The other quantities of interest are

$$\psi_0(\hat{\mathbf{r}})=\psi(\hat{\mathbf{r}};0)=\frac{1}{2\pi a}\int_0^{2\pi} d(a\phi')e^{ika|\hat{\mathbf{r}}-\hat{\mathbf{y}}|\cos\phi'}=J_0(2ka\sin(\phi/2-\pi/4)), \tag{3.2}$$

$$\sqrt{P(0)}=N(0)=\sum_{n=-\infty}^{\infty} J_n(ka)^2=1, \tag{3.3}$$

$$T(0)=\sum_{n=-\infty}^{\infty} J_n(ka)^4=T_0(ka). \tag{3.4}$$

A. Asymptotic formula for $T_0(ka)$

A convenient, alternative expression for $T_0(ka)$ is

$$T_0(ka)=\frac{1}{2\pi}\int_0^{2\pi} d\phi\,|\psi_0(\hat{\mathbf{r}})|^2=\frac{2}{\pi}\int_0^{\pi/2} d\theta\,J_0(2ka\sin\theta)^2. \tag{3.5}$$

Its Mellin transform reads[12,13]

$$\overline{T}_0(\zeta)=\int_0^\infty d(ka)\,(ka)^{-\zeta}T_0(ka)=2^{-\zeta}\frac{\Gamma(\zeta)^2\Gamma(\frac{1}{2}-\frac{1}{2}\zeta)}{\Gamma(\frac{1}{2}+\frac{1}{2}\zeta)^5}. \tag{3.6}$$

Note that for $\mathrm{Re}\,\zeta=c_0$ and $\mathrm{Im}\,\zeta=y\to\pm\infty$,

$$\overline{T}_0(\zeta)=\mathrm{O}(|y|^{-1-c_0}). \tag{3.7}$$

The inversion formula for $\overline{T}_0(\zeta)$ is

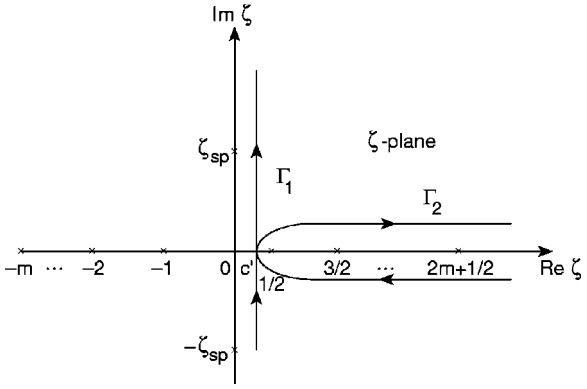

FIG. 4. Pole configuration for the integrand of Eq. (3.8) ($m=0, 1, 2, \ldots$). Γ_1 is the original inversion path in Eq. (3.8), and Γ_2 serves the evaluation of $T_0(ka)$ in terms of power series (3.33).

$$T_0(ka)=\frac{1}{2\pi i}\int_{c_0-i\infty}^{c_0+i\infty} d\zeta\, \overline{T}_0(\zeta)(ka)^{\zeta-1}, \quad 0<c_0<1$$

$$=\frac{1}{2\pi ka}\,\frac{1}{2\pi i}\int_{c'-i\infty}^{c'+i\infty} d\zeta\,\frac{\Gamma(\zeta)^2\Gamma(\frac{1}{2}-\zeta)}{\Gamma(\frac{1}{2}+\zeta)^3}(2ka)^{2\zeta}, \quad 0<c'<\tfrac{1}{2}, \tag{3.8}$$

where ζ is replaced by 2ζ in the first line and Legendre's duplication formula is invoked.

Equation (3.7) indicates that an asymptotic expansion of $T_0(ka)$ cannot be obtained by merely shifting the inversion contour in the left half of the ζ plane and calculating the relevant residues (see Fig. 4). Additional contributions come from two imaginary saddle points $\pm\zeta_{\rm sp}$ that give rise to oscillations in ka. To extract these oscillations, let

$$T_0(ka)=\frac{1}{\pi}\mathrm{Re}\int_0^{\pi/2} d\theta\, H_0^{(1)}(2ka\sin\theta)^2+\frac{1}{\pi}\int_0^{\pi/2} d\theta\, H_0^{(1)}(2ka\sin\theta)H_0^{(2)}(2ka\sin\theta). \tag{3.9}$$

Evaluation of the first integral is carried out along the positive imaginary axis and the axis $\mathrm{Re}\,\theta=\pi/2, \mathrm{Im}\,\theta>0$, as shown in Fig. 5:

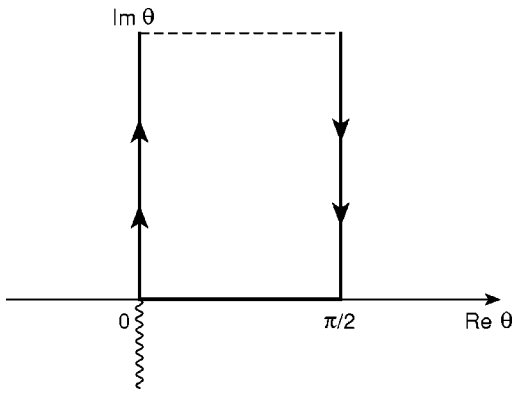

FIG. 5. Integration path (with arrows) for Eq. (3.10).

$$\int_0^{\pi/2} d\theta\, H_0^{(1)}(2ka\sin\theta)^2 = -i\frac{4}{\pi^2}\int_0^{\infty} dt\, K_0(2ka\sinh t)^2 - i\int_0^{\infty} dt\, H_0^{(1)}(2ka\cosh t)^2, \tag{3.10}$$

$$T_0(ka) = \mathrm{Im}\,\mathcal{I}_1(ka) + \mathcal{I}_2(ka), \tag{3.11}$$

$$\mathcal{I}_1(ka) = \frac{1}{\pi}\int_0^{\infty} dt\, H_0^{(1)}(2ka\cosh t)^2, \tag{3.12}$$

$$\mathcal{I}_2(ka) = \frac{1}{\pi}\int_0^{\pi/2} d\theta\,[J_0(2ka\sin\theta)^2 + Y_0(2ka\sin\theta)^2]. \tag{3.13}$$

For $ka \gg 1$, the major contribution to integration in $\mathcal{I}_1(ka)$ arises from the end point $t=0$, indicating that the resulting asymptotic expansion exhibits oscillations in ka. The situation is distinctly different for $\mathcal{I}_2(ka)$. These two cases are treated separately.

The change of variable $\mu = \sinh(t/2)e^{-i\pi/4}$ in $\mathcal{I}_1$, rotation of the integration path by $\pi/4$ in the counterclockwise sense, and use of the formula

$$H_0^{(1)}(x) = e^{i(x-\pi/4)}\sqrt{\frac{2}{\pi x}}\left[1 - \frac{i}{8x} - \frac{9}{128x^2} + \mathrm{O}\left(\frac{1}{x^3}\right)\right] \quad \text{as} \quad x\to\infty \tag{3.14}$$

result in retaining the first three terms of an asymptotic expansion for $\mathcal{I}_1$,

$$\mathcal{I}_1(ka) = \frac{2}{\pi}e^{i\pi/4}\int_0^{\infty} d\mu\,\frac{H_0^{(1)}(2ka(1+2i\mu^2))^2}{\sqrt{1+i\mu^2}} \sim (2\pi ka)^{-3/2}e^{i4ka - i\pi/4}\left[1 - \frac{9i}{32ka} - \frac{281}{2(32ka)^2}\right]. \tag{3.15}$$

This procedure can be readily carried out ad infinitum.

The evaluation of $\mathcal{I}_2(ka)$ is more involved. By use of the Mehler–Sonine formula[10]

$$Y_0(x) = -\frac{2}{\pi}\int_0^{\infty} dt\cos(x\cosh t), \quad x>0, \tag{3.16}$$

and the elementary integrals

$$\int_0^{\infty} dx\, x^{-\zeta}\cos x = \Gamma(1-\zeta)\sin(\pi\zeta/2), \quad 0<\mathrm{Re}\,\zeta<1, \tag{3.17a}$$

$$\int_0^{\infty} dt\,(\cosh t)^{\zeta-1} = \frac{\sqrt{\pi}}{2}\frac{\Gamma(\frac{1}{2}-\frac{1}{2}\zeta)}{\Gamma(1-\frac{1}{2}\zeta)}, \quad \mathrm{Re}\,\zeta<1, \tag{3.17b}$$

the Mellin transform of $Y_0(bx)$ $(b>0, x>0)$ is found to be

$$\int_0^{\infty} dx\, x^{-\zeta}Y_0(bx) = -\frac{b^{\zeta-1}}{\sqrt{\pi}}\sin(\pi\zeta/2)\frac{\Gamma(1-\zeta)\Gamma(\frac{1}{2}-\frac{1}{2}\zeta)}{\Gamma(1-\frac{1}{2}\zeta)}. \tag{3.18}$$

The combination of this result with the known formula[10]

$$J_0(x)^2 - Y_0(x)^2 = \frac{4}{\pi}\int_0^{\infty} dt\, Y_0(2x\cosh t) \tag{3.19}$$

and Eq. (3.17b) yields

$$\int_0^\infty dx\, x^{-\zeta}[J_0(x)^2 - Y_0(x)^2] = \sin(\pi\zeta/2)\overline{\mathcal{I}}(\zeta), \tag{3.20}$$

$$\overline{\mathcal{I}}(\zeta) = -\frac{1}{\pi} 2^{\zeta} \frac{\Gamma(1-\zeta)\Gamma(\frac{1}{2}-\frac{1}{2}\zeta)^2}{\Gamma(1-\frac{1}{2}\zeta)^2}. \tag{3.21}$$

Note that $\overline{\mathcal{I}}(\zeta)$ is holomorphic for $\mathrm{Re}\,\zeta<0$.

It follows from Eqs. (3.13) and (3.20) and the integral

$$\int_0^{\pi/2} d\theta\, (\sin\theta)^{\zeta-1} = \frac{\sqrt{\pi}}{2} \frac{\Gamma(\frac{1}{2}\zeta)}{\Gamma(\frac{1}{2}+\frac{1}{2}\zeta)} \tag{3.22}$$

that the Mellin transform of $\mathcal{I}_2(ka)$ equals

$$\begin{aligned}\overline{\mathcal{I}}_2(\zeta) &= \int_0^\infty d(ka)\,(ka)^{-\zeta}\mathcal{I}_2(ka), \quad 0<\mathrm{Re}\,\zeta<1 \\ &= -\sqrt{\pi}\frac{2^{\zeta-2}}{\Gamma(1-\frac{1}{2}\zeta)\Gamma(\frac{1}{2}+\frac{1}{2}\zeta)}\overline{\mathcal{I}}(\zeta) + \overline{T}_0(\zeta) \\ &= \pi^{-3}2^{\zeta-2}\frac{\Gamma(\frac{1}{2}-\frac{1}{2}\zeta)^3\Gamma(\frac{1}{2}\zeta)^2}{\Gamma(\frac{1}{2}+\frac{1}{2}\zeta)},\end{aligned} \tag{3.23}$$

$$\overline{\mathcal{I}}_2(\zeta) = \mathrm{O}(|y|^{-1-c_0}e^{-\pi|y|}), \quad \mathrm{Re}\,\zeta = c_0, \quad \mathrm{Im}\,\zeta = y \to \pm\infty. \tag{3.24}$$

$\overline{\mathcal{I}}_2(\zeta) - \overline{T}_0(\zeta)$ is holomorphic for $\mathrm{Re}\,\zeta<0$. Compare with Eq. (3.7).

Evidently, $\overline{\mathcal{I}}_2(\zeta)$ has double poles at $\zeta_{m-} = -2m$ $(m=0,1,2,\ldots)$. In view of Eq. (3.24), an asymptotic expansion of $\mathcal{I}_2(ka)$ can be obtained by merely shifting the contour in the left half of the ζ plane and summing the relevant residues. In the vicinity of each ζ_{m-},[14]

$$\begin{aligned}\overline{\mathcal{I}}_2(\zeta)(ka)^{\zeta-1} \sim \frac{1}{2}\left(\frac{ka}{2}\right)^{-2m-1} &\frac{\Gamma(\frac{1}{2}+m)}{(2m)!^2\Gamma(\frac{1}{2}-m)^5}\left\{\frac{1}{(\zeta-\zeta_{m-})^2} + [2\psi(1+2m) - 3\psi(\tfrac{1}{2}+m)\right. \\ &\left. + \ln(ka/2)]\frac{1}{\zeta-\zeta_{m-}}\right\},\end{aligned} \tag{3.25}$$

$$\psi(z) = \frac{d}{dz}\ln\Gamma(z), \quad \psi(1+z) = \frac{1}{z} + \psi(z), \tag{3.26}$$

$$\psi(1) = -\gamma = -0.577\,215\,664\,9\cdots, \quad \psi(\tfrac{1}{2}) = -\gamma - 2\ln 2. \tag{3.27}$$

Hence, for $ka \gg 1$ and positive integer M,

$$\begin{aligned}\mathcal{I}_2(ka) &= \frac{1}{2\pi i}\int_{c_0-i\infty}^{c_0+i\infty} d\zeta\, \overline{\mathcal{I}}_2(\zeta)(ka)^{\zeta-1}, \quad 0<c_0<1 \\ &\sim \frac{1}{\pi^2 ka}\sum_{m=0}^{M-1}\left(\frac{2}{ka}\right)^{2m}\frac{(-1)^m}{(2m)!^2}\left(\frac{1}{2}\right)_m^6[2\psi(1+2m) - 3\psi(\tfrac{1}{2}+m) + \ln(ka/2)],\end{aligned} \tag{3.28}$$

where $(a)_m$ is Pochhammer's symbol, i.e.,

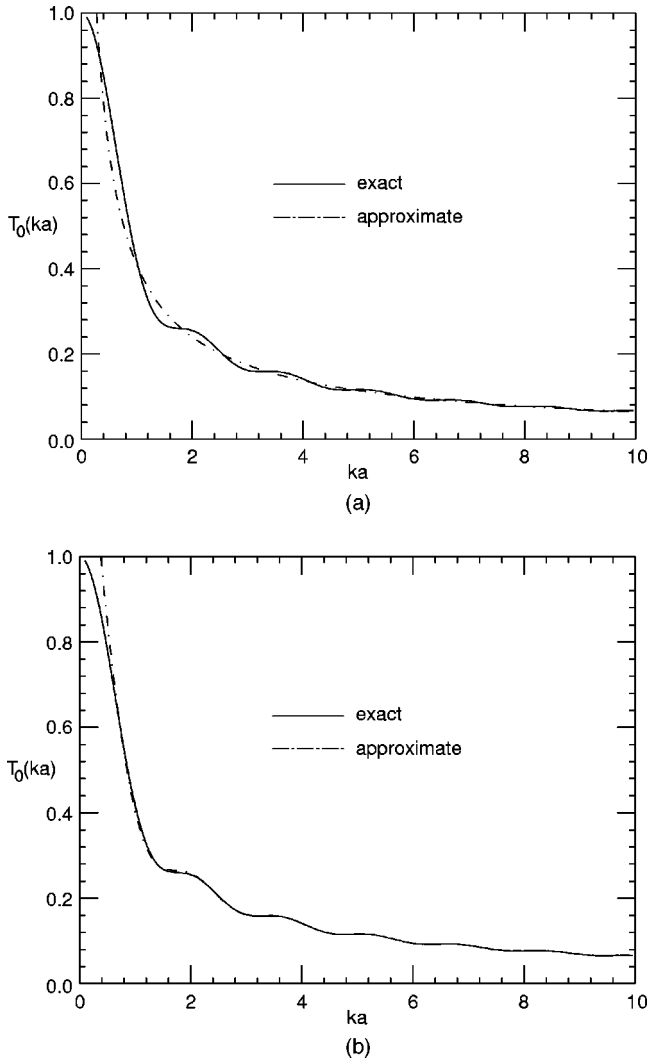

FIG. 6. (a) Comparison of the exact series (3.4) with the term $[\gamma+\ln(32ka)]/(\pi^2 ka)$ of approximate formula (3.30). (b) Comparison of the exact series (3.4) with the first two terms (including the cosine) of approximate formula (3.30).

$$(\mathrm{a})_0=1, \quad (\mathrm{a})_m=\mathrm{a}(\mathrm{a}+1)\cdots(\mathrm{a}+m-1), \quad m=1,2,\ldots . \tag{3.29}$$

An asymptotic formula for $T_0(ka)$ follows from Eqs. (3.11), (3.15), and (3.28) with Eqs. (3.26), (3.27), and (3.29) and $M=2$:

$$T_0(ka)\sim \frac{\ln(32ka)+\gamma}{\pi^2 ka}-\frac{1}{(2\pi ka)^{3/2}}\cos(4ka+\pi/4)-\frac{9\pi}{16(2\pi ka)^{5/2}}\sin(4ka+\pi/4)$$
$$-\frac{\ln(32ka)-3+\gamma}{64\pi^2(ka)^3}+\frac{281\pi^2}{512(2\pi ka)^{7/2}}\cos(4ka+\pi/4). \tag{3.30}$$

Compare with Ref. 15. The first three terms of this asymptotic formula (up to the first cosine) provide remarkable accuracy even for low values of ka ($ka\geqslant 0.5$). See Figs. 6(a) and 6(b) for comparisons with the numerically computed exact series. The corresponding formula for $C_0=N_0/T_0$ and $D_0=P_0/T_0$ is

$$C_0 = D_0 \sim \frac{\pi^2 ka}{\gamma + \ln(32ka)} \left\{ 1 + \frac{\pi}{2} \frac{\cos(4ka + \pi/4)}{(ka)^{1/2}[\gamma + \ln(32ka)]} \right\}, \quad ka \gg 1. \tag{3.31}$$

B. Exact formula for $T_0(ka)$

In Eq. (3.8), allow the original integration path to envelope the positive real axis (Fig. 4). In the vicinity of each simple pole $\zeta_{m+} = m + \frac{1}{2}$ $(m = 0,1,2,\ldots)$,

$$\frac{\Gamma(\zeta)^2 \Gamma(\frac{1}{2} - \zeta)}{\Gamma(\frac{1}{2} + \zeta)^3} \sim \frac{(-1)^{m+1}}{m!} \frac{\Gamma(m + \frac{1}{2})^2}{\Gamma(m+1)^3} \frac{1}{\zeta - \zeta_{m+}}. \tag{3.32}$$

The evaluation and summation of the residues give

$$T_0(ka) = \frac{1}{\pi} \sum_{m=0}^{\infty} \frac{\Gamma(m + \frac{1}{2})^2}{(m!)^4} (-4k^2a^2)^m = {}_2F_3(\tfrac{1}{2}, \tfrac{1}{2}; 1,1,1; -4k^2a^2). \tag{3.33}$$

${}_2F_3$ is a hypergeometric series.[16]

IV. POWER FLUX $P(\alpha)$

A. Case $\alpha \ll ka$

For $0 \leqslant \alpha \ll ka$, series (2.22) is recast in the form[17,18]

$$\sqrt{P(\alpha)} = 1 - \alpha T_0(ka) + 2\alpha^2 \sum_{n=0}^{\infty} \frac{J_n(ka)^6}{1 + \alpha J_n(ka)^2} - \alpha^2 \frac{J_0(ka)^6}{1 + \alpha J_0(ka)^2} \tag{4.1}$$

$$\sim 1 - \alpha T_0(ka) + 2\left(\frac{2}{ka}\right)^{1/3} \tilde{\alpha}^2 G_{\mathrm{P}}(\tilde{\alpha}) \quad \text{as} \quad ka \to \infty, \tag{4.2}$$

where

$$\tilde{\alpha} = \alpha \left(\frac{ka}{2}\right)^{-2/3}, \tag{4.3}$$

$$G_{\mathrm{P}}(x) = \int_{-\infty}^{\infty} d\xi \frac{\mathrm{Ai}(\xi)^6}{1 + x\ \mathrm{Ai}(\xi)^2}, \quad x > 0. \tag{4.4}$$

By virtue of expansion (3.30),

$$\sqrt{P(\alpha)} = 1 - \alpha \frac{\ln ka}{\pi^2 ka} + \mathrm{O}\left(\frac{\alpha}{ka}\right), \quad \tilde{\alpha} \leqslant \mathrm{O}(1). \tag{4.5}$$

If α is scaled as α/ka, the leading term of the asymptotic expansion for G_{P} produces a term that exactly cancels the logarithm (see Appendix B). It follows from approximation (4.2) and Eq. (C48) of Appendix C that

$$\sqrt{P(\alpha)} \sim 1 - \frac{3}{\pi^2} \frac{\alpha}{ka} \ln \frac{ka}{\alpha} - \frac{3\ln(4\pi) - \frac{7}{2}}{\pi^2} \frac{\alpha}{ka}, \quad \tilde{\alpha} \gg 1, \quad \alpha \ll ka. \tag{4.6}$$

This expansion breaks down when $\alpha = \mathrm{O}(ka)$.

B. $\alpha = O(ka)$

In view of decomposition (2.34), the integrand of Eq. (2.27) for $m=0$ is written as

$$\frac{J_\nu(ka)^2}{1+\alpha J_\nu(ka)^2} = F_{\mathrm{P}}^{(\mathrm{osc})}(\nu) + F_{\mathrm{P}}^{(\mathrm{nos})}(\nu). \tag{4.7}$$

The $F_{\mathrm{P}}^{(\mathrm{osc})}$ defined as

$$F_{\mathrm{P}}^{(\mathrm{osc})}(\nu) = \frac{1+\tau_1^2 AB}{\tau_2^2+\alpha AB}\left[\frac{A^2}{1-(\tau_1 A)^2}+\frac{B^2}{1-(\tau_1 B)^2}\right] \tag{4.8}$$

is oscillatory in ν when $0<\nu<ka$. In contrast, the $F_{\mathrm{P}}^{(\mathrm{nos})}$ given by

$$F_{\mathrm{P}}^{(\mathrm{nos})}(\nu) = \frac{2AB}{\tau_2^2+\alpha AB} \tag{4.9}$$

is not oscillatory to the leading order in $(ka)^{-1}$.

Accordingly,

$$\sqrt{P(\alpha)} = 2\sum_{m=-\infty}^{\infty}[\mathcal{I}_{\mathrm{P}<,m}^{(\mathrm{osc})}(\alpha)+\mathcal{I}_{\mathrm{P}<,m}^{(\mathrm{nos})}(\alpha)+\mathcal{I}_{\mathrm{P}>,m}(\alpha)], \tag{4.10}$$

$$\mathcal{I}_{\mathrm{P}<,m}^{(\mathrm{osc})}(\alpha) = \int_0^{ka} d\nu\, F_{\mathrm{P}}^{(\mathrm{osc})}(\nu) e^{i2\pi m\nu}, \tag{4.11}$$

$$\mathcal{I}_{\mathrm{P}<,m}^{(\mathrm{nos})}(\alpha) = \int_0^{ka} d\nu\, F_{\mathrm{P}}^{(\mathrm{nos})}(\nu) e^{i2\pi m\nu}, \tag{4.12}$$

$$\mathcal{I}_{\mathrm{P}>,m}(\alpha) = \int_{ka}^{\infty} d\nu \frac{J_\nu(ka)^2}{1+\alpha J_\nu(ka)^2} e^{i2\pi m\nu}. \tag{4.13}$$

The inspection of the $m\neq 0$ terms suggests that[18]

$$\sqrt{P(\alpha)} \sim 2\,[\mathcal{I}_{\mathrm{P}<,m=0}^{(\mathrm{nos})}(\alpha)+\mathcal{I}_{\mathrm{P}>,m=0}(\alpha)], \tag{4.14}$$

which is useful for all $\alpha \geqslant 0$.

In particular, for $\alpha = O(ka)$,

$$\sqrt{P(\alpha)} \sim 2\mathcal{I}_{\mathrm{P}<,m=0}^{(\mathrm{nos})}(\alpha). \tag{4.15}$$

This approximation can be justified heuristically by noticing that the width of the critical integration range in formula (4.14) is roughly determined by the condition

$$\alpha J_\nu(ka)^2 = O(1). \tag{4.16}$$

According to Ref. 10,

$$F_{\mathrm{P}}^{(\mathrm{nos})}(\nu) \sim \frac{1}{\alpha}\left\{1-\frac{1}{\sqrt{1+\overline{\alpha}[1-(\nu/ka)]^{-1/2}}}\right\}, \tag{4.17}$$

where

$$\overline{\alpha}=\frac{2\alpha}{\pi ka}. \tag{4.18}$$

It follows from Eq. (4.12) that

$$\mathcal{I}^{(\mathrm{nos})}_{\mathrm{P}<,m=0}(\alpha)=\frac{ka}{\alpha}\left[1-\int_0^1\frac{dx}{\sqrt{1+4\alpha A(kax)B(kax)}}\right] \tag{4.19}$$

$$\sim\frac{2}{\pi\overline{\alpha}}[1-Z_{\mathrm{P}}(\overline{\alpha})], \tag{4.20}$$

$$Z_{\mathrm{P}}(\overline{\alpha})=\int_0^1 dx\,\frac{(1-x^2)^{1/4}}{[(1-x^2)^{1/2}+\overline{\alpha}]^{1/2}}. \tag{4.21}$$

With the change of variable $x=2t/(1+t^2)$,

$$Z_{\mathrm{P}}(\overline{\alpha})=\frac{2}{\sqrt{1+\overline{\alpha}}}\int_0^1 dt\,\frac{(1-t^2)^2}{(1+t^2)^2}\,\frac{1}{\sqrt{(1-t^2)(1-\kappa^2t^2)}}, \tag{4.22}$$

$$\kappa^2=\frac{1-\overline{\alpha}}{1+\overline{\alpha}}. \tag{4.23}$$

$Z_{\mathrm{P}}(\overline{\alpha})$ is evaluated in terms of the complete elliptic integrals $\mathbf{E}$ and Π_1 as follows.[10]

Consider each one of the two integrals arising from the decomposition

$$\frac{(1-t^2)^2}{(1+t^2)^2}=-\frac{2}{1+t^2}+\frac{(1+t^2)^2+2(1-t^2)}{(1+t^2)^2}. \tag{4.24}$$

The first integral is identified with $\Pi_1(1,\kappa)$. In view of the identity

$$\frac{d}{dt}\left[t\,\frac{\sqrt{(1-t^2)(1-\kappa^2t^2)}}{1+t^2}\right]=\frac{1}{\sqrt{(1-t^2)(1-\kappa^2t^2)}}\times\left[2(1+\kappa^2)\,\frac{1-t^2}{(1+t^2)^2}-\frac{1+3\kappa^2}{1+t^2}+2\kappa^2-\kappa^2(1-t^2)\right], \tag{4.25}$$

the second integral is evaluated as

$$\int_0^1\frac{dt}{(1+t^2)^2}\,\frac{(1+t^2)^2+2(1-t^2)}{\sqrt{(1-t^2)(1-\kappa^2t^2)}}=\frac{1+3\kappa^2}{1+\kappa^2}\,\Pi_1(1,\kappa)+\frac{1}{1+\kappa^2}\,\mathbf{E}(\kappa). \tag{4.26}$$

Equation (4.21) then gives

$$Z_{\mathrm{P}}(\overline{\alpha})=\sqrt{1+\overline{\alpha}}[\mathbf{E}(\kappa)-(1-\kappa^2)\Pi_1(1,\kappa)]. \tag{4.27}$$

With approximation (4.20) and $\overline{\alpha}=\mathrm{O}(1)$,

$$\mathcal{I}^{(\mathrm{nos})}_{\mathrm{P}<,m=0}(\alpha)\sim\frac{2}{\pi\overline{\alpha}}\{1-\sqrt{1+\overline{\alpha}}[\mathbf{E}(\kappa)-(1-\kappa^2)\Pi_1(1,\kappa)]\}. \tag{4.28}$$

It is easily verified that this formula can be extended to $\alpha\gg ka$, when $Z_{\mathrm{P}}(\overline{\alpha})$ becomes of the order of $1/\sqrt{\overline{\alpha}}$. From expression (4.15),

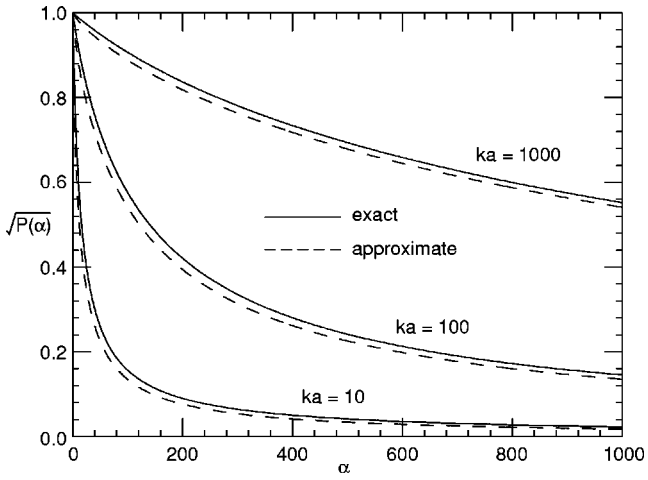

FIG. 7. Comparison of the exact series (2.22) for $\sqrt{P(\alpha)}$ with approximate formula (4.29).

$$\sqrt{P(\alpha)}\sim\frac{4}{\pi\overline{\alpha}}\{1-\sqrt{1+\overline{\alpha}}[\mathbf{E}(\kappa)-(1-\kappa^2)\Pi_1(1,\kappa)]\},\quad \overline{\alpha}\ll O(1). \tag{4.29}$$

This formula is compared with the original exact series (2.22) in Fig. 7. It is verified that α scales as $\alpha/(ka)$.

It remains to check whether the preceding formula connects smoothly to expansion (4.6). Indeed, with $\kappa'=\sqrt{1-\kappa^2}$ and the expansions

$$\mathbf{E}(\kappa)=1+\frac{1}{2}\left(\ln\frac{4}{\kappa'}-\frac{1}{2}\right)\kappa'^2+\frac{3}{16}\left(\ln\frac{4}{\kappa'}-\frac{13}{12}\right)\kappa'^4+O\left(\kappa'^6\ln\frac{1}{\kappa'}\right), \tag{4.30}$$

$$\Pi_1(1,\kappa)=\frac{1}{2}\ln\frac{4}{\kappa'}+\frac{\pi}{8}+\frac{\pi-2}{32}\kappa'^2+O\left(\kappa'^4\ln\frac{1}{\kappa'}\right)\quad \text{as}\quad \kappa'\to 0^+, \tag{4.31}$$

it becomes evident that (4.29) reproduces all three terms of expansion (4.6).

C. Considerations for $\alpha > O(ka)$

It is worthwhile noting that

$$\mathcal{I}^{(\mathrm{nos})}_{\mathrm{P}<,m=0}(\alpha)=O(ka/\alpha),\quad \alpha\gg ka. \tag{4.32}$$

Condition (4.16) indicates that the integral $\mathcal{I}_{\mathrm{P}>,m=0}$ of formula (4.14) should be invoked.

For sufficiently large α, the principal contribution to integration in $\mathcal{I}_{\mathrm{P}>,m=0}$ arises from a range outside the transitional region for the Bessel function.[10] Accordingly,

$$\mathcal{I}_{\mathrm{P}>,m=0}(\alpha)\sim I_{\mathrm{P}}(\alpha), \tag{4.33}$$

where

$$I_{\mathrm{P}}(\alpha)=\frac{ka}{\alpha}\int_1^\infty\frac{d\eta}{\sqrt{\eta^2-1}}\frac{e^{2ka[\Lambda-\Phi(\eta)]}}{1+(\eta^2-1)^{-1/2}e^{2ka[\Lambda-\Phi(\eta)]}}, \tag{4.34}$$

$$\Phi(\eta)=\eta\ln(\eta+\sqrt{\eta^2-1})-\sqrt{\eta^2-1}, \tag{4.35}$$

$$\Lambda = \frac{1}{2ka} \ln \frac{\alpha}{2\pi ka}. \tag{4.36}$$

The analysis is facilitated by introduction of the variable

$$\varsigma = \Phi(\eta) + \frac{1}{4ka} \ln(\eta^2 - 1), \quad \eta = \eta(\varsigma). \tag{4.37}$$

The major contribution to integration arises from $\varsigma = O(\Lambda)$ with a width $O[(ka)^{-1}]$. It is found through differentiation of both sides of the preceding equation that when

$$|\Lambda| = O\left(\frac{\ln ka}{ka}\right), \quad \Lambda < 0, \tag{4.38}$$

$\eta(\Lambda) - 1$ becomes of the order of $(ka)^{-2/3}$, and the integration in Eq. (4.13) for $m = 0$ needs to take into account the transitional region of the Bessel function. Then formula (4.33) apparently breaks down. This remains a reasonable approximation if

$$0 \leqslant -\Lambda \ll \frac{\ln ka}{ka}$$

or

$$\Lambda > 0. \tag{4.39}$$

In some detail,

$$\begin{aligned} I_P(\alpha) &= \frac{ka}{\alpha} \int_{-\infty}^{\infty} d\varsigma\, \eta'(\varsigma) \frac{e^{2ka(\Lambda - \varsigma)}}{1 + e^{2ka(\Lambda - \varsigma)}} \\ &= \frac{ka}{\alpha}[\eta(\Lambda) - 1] + \frac{1}{2\alpha} \int_0^{\infty} dt \left[\eta'\left(\Lambda + \frac{t}{2ka}\right) - \eta'\left(\Lambda - \frac{t}{2ka}\right) \right] \frac{1}{1 + e^t} \\ &\sim \frac{ka}{\alpha}[\eta(\Lambda) - 1] + \frac{\pi^2}{24\alpha ka} \eta''(\Lambda), \quad ka \gg 1, \quad ka\Lambda \gg 1, \end{aligned} \tag{4.40}$$

where the prime here denotes differentiation with respect to the argument. The following three cases are distinguished for Λ.

1. $\Lambda \gg 1$

Starting with the asymptotic expansion

$$\varsigma(\eta) = \eta \ln \frac{2\eta}{e} + 2 \frac{\ln \eta}{ka} + \frac{3}{4\eta} - \frac{1}{4ka\,\eta^2} + O(1/\eta^3) \quad \text{as} \quad \eta \to \infty, \tag{4.41}$$

define an $\eta_0 = \eta_0(\varsigma)$ such that

$$\varsigma = \eta_0 \ln \frac{2\eta_0}{e}. \tag{4.42}$$

If terms of the order of $1/\eta^2$ or smaller are neglected in expansion (4.41), then

$$\eta(\Lambda)\sim\eta_0(\Lambda)-\frac{2}{ka}\,\eta_0'(\Lambda)\ln\eta_0(\Lambda)-\frac{3}{4}\,\frac{\eta_0'(\Lambda)}{\eta_0(\Lambda)},\quad \Lambda\gg 1. \tag{4.43}$$

Through successive iterations of Eq. (4.42),

$$\eta_0(\Lambda)=\frac{\Lambda}{\ln(2\Lambda/e)}\left\{1+\frac{\ln\overline{\Lambda}}{\overline{\Lambda}}+\frac{(\ln\overline{\Lambda})^2-\ln\overline{\Lambda}}{\overline{\Lambda}^2}+\frac{(\ln\overline{\Lambda})^3-(5/2)(\ln\overline{\Lambda})^2+\ln\overline{\Lambda}}{\overline{\Lambda}^3}\right.$$
$$\left.+\frac{(\ln\overline{\Lambda})^4-(13/3)(\ln\overline{\Lambda})^3+(9/2)(\ln\overline{\Lambda})^2-\ln\overline{\Lambda}}{\overline{\Lambda}^4}+\mathrm{O}\left[\frac{(\ln\overline{\Lambda})^5}{\overline{\Lambda}^5}\right]\right\}, \tag{4.44}$$

$$\eta_0'(\Lambda)=\frac{1}{\ln[2\,\eta_0(\Lambda)]}=\frac{1}{\overline{\Lambda}}+\frac{\ln\overline{\Lambda}-1}{\overline{\Lambda}^2}+\frac{(\ln\overline{\Lambda})^2-3\ln\overline{\Lambda}+1}{\overline{\Lambda}^3}$$
$$+\frac{(\ln\overline{\Lambda})^3-(11/2)(\ln\overline{\Lambda})^2+6\ln\overline{\Lambda}-1}{\overline{\Lambda}^4}+\mathrm{O}\left[\frac{(\ln\overline{\Lambda})^4}{\overline{\Lambda}^5}\right], \tag{4.45}$$

$$\eta_0''(\Lambda)=\mathrm{O}\left[\frac{1}{\Lambda(\ln\Lambda)^2}\right]\quad\text{as}\quad\Lambda\to\infty, \tag{4.46}$$

where

$$\overline{\Lambda}=\ln\frac{2\Lambda}{e}. \tag{4.47}$$

An asymptotic formula for I_{P} ensues from expansion (4.40):

$$I_{\mathrm{P}}\sim\frac{ka}{\alpha}[\,\eta_0(\Lambda)-1]. \tag{4.48}$$

In particular,

$$\mathcal{I}_{\mathrm{P}>,m=0}(\alpha)=\frac{1}{2\alpha}\,\frac{\ln\alpha}{\ln\ln\alpha}\left\{1+\frac{\ln\ln\ln\alpha}{\ln\ln\alpha}+\mathrm{O}\left[\left(\frac{\ln\ln\ln\alpha}{\ln\ln\alpha}\right)^2\right]\right\}\quad\text{as}\quad\alpha\to\infty. \tag{4.49}$$

2. $\Lambda=\mathrm{O}(1)$

Clearly,

$$I_{\mathrm{P}}(\alpha)=\frac{ka}{\alpha}[\,\eta(\Lambda)-1]+\mathrm{O}[(\alpha ka)^{-1}], \tag{4.50}$$

where

$$\Lambda\sim\eta\ln(\eta+\sqrt{\eta^2-1})-(\eta^2-1)^{1/2}. \tag{4.51}$$

This approximate equation for η can be solved numerically for fixed Λ.

3. $1 \ll ka\Lambda \ll ka$

For $(ka)^{2/5}(\ln ka)^{3/5} \ll ka\Lambda \ll ka$, the term

$$\frac{1}{4ka}\ln(\eta^2-1)$$

can be neglected in Eq. (4.37):

$$I_{\mathrm{P}}(\alpha) \sim \frac{ka}{\alpha}[\eta(\Lambda)-1] = \frac{ka}{\alpha}\left[\frac{1}{2}(3\Lambda)^{2/3}+\mathrm{O}(\Lambda^{4/3})\right]. \tag{4.52}$$

For $1 \ll ka\Lambda \ll (ka)^{2/5}(\ln ka)^{3/5}$, the previously neglected logarithm needs to be taken into account. The scaling

$$\xi = 2^{1/3}(ka)^{2/3}(\eta-1), \quad \tilde{\Lambda} = 3ka\Lambda/2, \quad \xi = \xi(\varsigma) > 0, \tag{4.53}$$

leads to

$$\xi(\Lambda)^{3/2} + \tfrac{3}{8}\ln\xi(\Lambda) \sim \tilde{\Lambda}, \quad \tilde{\Lambda} \gg 1, \tag{4.54}$$

which in turn gives

$$\xi(\Lambda) \sim \tilde{\Lambda}^{2/3}[1 - \tfrac{1}{6}\tilde{\Lambda}^{-1}\ln\tilde{\Lambda} - \tfrac{1}{144}\tilde{\Lambda}^{-2}(\ln\tilde{\Lambda})^2 + \tfrac{1}{24}\tilde{\Lambda}^{-2}\ln\tilde{\Lambda}]. \tag{4.55}$$

$I_{\mathrm{P}}(\alpha)$ is readily evaluated from approximation (4.40) with the neglect of $\eta''(\Lambda)$.

D. Asymptotic formula for $P(\alpha)$

The foregoing discussion suggests that the integrals $\mathcal{I}^{(\mathrm{nos})}_{\mathrm{P}<,m=0}$ and $\mathcal{I}_{\mathrm{P}>,m=0}$ become of the same order in magnitude when $0<\Lambda=\mathrm{O}(1)$, the second one dominating when $\Lambda \gg 1$. The leading term for $\sqrt{P(\alpha)}$ is

$$\sqrt{P(\alpha)} \sim \frac{2ka}{\alpha}\{1-\sqrt{1+\overline{\alpha}}[\mathbf{E}(\kappa)-(1-\kappa^2)\Pi_1(1,\kappa)]+[\eta(\Lambda)-1]\}, \tag{4.56}$$

to all orders in α, where

$$\varsigma = \eta(\varsigma)\ln[\eta(\varsigma)+\sqrt{\eta(\varsigma)^2-1}] - \sqrt{\eta(\varsigma)^2-1} + \frac{1}{4ka}\ln[\eta(\varsigma)^2-1]. \tag{4.57}$$

$\overline{\alpha}$, κ, and Λ are defined by Eqs. (4.18), (4.23), and (4.36).

V. CURRENT NORM

The asymptotic analysis for $N(\alpha)$ is quite similar to that for $\sqrt{P(\alpha)}$.

A. Case $\alpha \ll ka$

The exact series (2.23) is recast in the form

$$N(\alpha) = 1 - 2\alpha T_0(ka) + 2\alpha^2\left\{2\sum_{n=0}^{\infty}\frac{J_n(ka)^6}{1+\alpha J_n(ka)^2} + \sum_{n=0}^{\infty}\frac{J_n(ka)^6}{[1+\alpha J_n(ka)^2]^2}\right\}$$
$$- \alpha^2 J_0(ka)^6\frac{3+2\alpha J_0(ka)^2}{[1+\alpha J_0(ka)^2]^2}$$

$$\sim 1-2\alpha T_0(ka)+2\left(\frac{2}{ka}\right)^{1/3}\tilde{\alpha}^2[2G_{\mathrm{P}}(\tilde{\alpha})+G_{\mathrm{N}}(\tilde{\alpha})], \tag{5.1}$$

where

$$G_{\mathrm{N}}(x)=\int_{-\infty}^{\infty} d\xi \frac{\mathrm{Ai}(\xi)^6}{[1+x\mathrm{Ai}(\xi)^2]^2}, \quad x>0. \tag{5.2}$$

$\tilde{\alpha}$ and $G_{\mathrm{P}}(x)$ are defined by Eqs. (4.3) and (4.4). In analogy with Eq. (4.5) and expansion (4.6),

$$N(\alpha)=1-2\alpha\frac{\ln ka}{\pi^2 ka}+\mathrm{O}\left(\frac{\alpha}{ka}\right), \quad \tilde{\alpha}\leqslant \mathrm{O}(1), \tag{5.3}$$

$$N(\alpha)\sim 1-\frac{6}{\pi^2}\frac{\alpha}{ka}\ln\frac{ka}{\alpha}-\frac{6\ln(4\pi)-10}{\pi^2}\frac{\alpha}{ka}, \quad \tilde{\alpha}\gg 1, \quad \alpha\ll ka. \tag{5.4}$$

B. $\alpha=\mathrm{O}(ka)$

In consideration of decomposition (2.34), let

$$\frac{J_\nu(ka)^2}{[1+\alpha J_\nu(ka)^2]^2}=F_{\mathrm{N}}^{(\mathrm{osc})}(\nu)+F_{\mathrm{N}}^{(\mathrm{nos})}(\nu), \tag{5.5}$$

where

$$F_{\mathrm{N}}^{(\mathrm{osc})}(\nu)=\frac{1}{(\tau_2^2+\alpha AB)^2}\left\{\frac{A^2}{[1-(\tau_1 A)^2]^2}+\frac{2AB}{1-(\tau_1^2AB)^2}\frac{(\tau_1A)^2}{1-(\tau_1A)^2}+\frac{B^2}{[1-(\tau_1B)^2]^2}\right.$$
$$\left.+\frac{2AB}{1-(\tau_1^2AB)^2}\frac{(\tau_1B)^2}{1-(\tau_1B)^2}\right\}, \tag{5.6}$$

$$F_{\mathrm{N}}^{(\mathrm{nos})}(\nu)=\frac{2AB}{(\tau_2^2+\alpha AB)^2}\frac{1}{1-(\tau_1^2AB)^2}. \tag{5.7}$$

$\tau_{1,2}$ are defined by Eq. (2.33). With the definitions[18]

$$\mathcal{I}_{\mathrm{N}<,m}^{(\mathrm{osc})}(\alpha)=\int_0^{ka} d\nu F_{\mathrm{N}}^{(\mathrm{osc})}(\nu)e^{i2\pi m\nu}, \tag{5.8}$$

$$\mathcal{I}_{\mathrm{N}<,m}^{(\mathrm{nos})}(\alpha)=\int_0^{ka} d\nu F_{\mathrm{N}}^{(\mathrm{nos})}(\nu)e^{i2\pi m\nu}, \tag{5.9}$$

$$\mathcal{I}_{\mathrm{N}>,m}(\alpha)=\int_{ka}^{\infty} d\nu \frac{J_\nu(ka)^2}{[1+\alpha J_\nu(ka)^2]^2}e^{i2\pi m\nu}, \tag{5.10}$$

it is evident that only $\mathcal{I}_{\mathrm{N}<,m=0}^{(\mathrm{nos})}$ and $\mathcal{I}_{\mathrm{N}>,m=0}$ contribute to the lowest order in $(ka)^{-1}$:

$$N(\alpha)\sim 2[\mathcal{I}_{\mathrm{N}<,m=0}^{(\mathrm{nos})}(\alpha)+\mathcal{I}_{\mathrm{N}>,m=0}(\alpha)]. \tag{5.11}$$

Now consider $\alpha=\mathrm{O}(ka)$. By analogy with Eq. (4.20),

$$\mathcal{I}_{\mathrm{N}<,m=0}^{(\mathrm{nos})}(\alpha)\sim \pi^{-1}Z_{\mathrm{N}}(\overline{\alpha}), \tag{5.12}$$

where

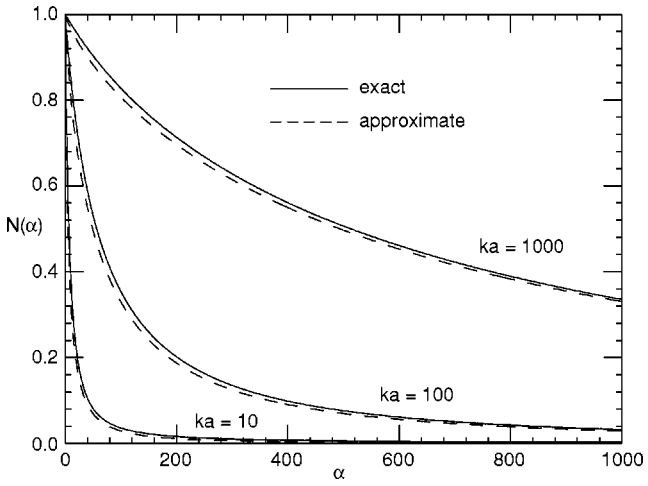

FIG. 8. Comparison of the exact series (2.23) for $N(\alpha)$ with approximate formula (5.17).

$$Z_{\mathrm{N}}(\overline{\alpha})=\frac{2}{(1+\overline{\alpha})^{3/2}}\int_0^1 dt\,\frac{(1-t^2)^2}{(1+t^2)(1-\kappa^2t^2)}\,\frac{1}{\sqrt{(1-t^2)(1-\kappa^2t^2)}}, \tag{5.13}$$

and $\overline{\alpha}$ and κ are defined by Eqs. (4.18) and (4.23). The use of the equalities

$$\frac{(1-t^2)^2}{(1+t^2)(1-\kappa^2t^2)}=-\frac{1}{\kappa^2}+\frac{4}{1+\kappa^2}\,\frac{1}{1+t^2}+\frac{(1-\kappa^2)^2}{\kappa^2(1+\kappa^2)}\,\frac{1}{1-\kappa^2t^2} \tag{5.14}$$

and

$$\frac{d}{dt}\left(t\sqrt{\frac{1-t^2}{1-\kappa^2t^2}}\right)=\frac{1}{\kappa^2}\sqrt{\frac{1-\kappa^2t^2}{1-t^2}}-\frac{1-\kappa^2}{\kappa^2}\,\frac{1}{(1-\kappa^2t^2)\sqrt{(1-t^2)(1-\kappa^2t^2)}} \tag{5.15}$$

yields

$$Z_{\mathrm{N}}(\overline{\alpha})=\frac{2}{\sqrt{1+\overline{\alpha}}}\left[2\Pi_1(1,\kappa)-\frac{\mathbf{K}(\kappa)-\overline{\alpha}\mathbf{E}(\kappa)}{1-\overline{\alpha}}\right], \tag{5.16}$$

where $\mathbf{K}$ is the complete elliptic integral of the first kind.[10] $\mathcal{I}^{(\mathrm{nos})}_{\mathrm{N}<,m=0}(\alpha)$ is evaluated from formula (5.12). This formula can be extended to $\alpha\gg ka$.

The ensuing leading term for $N(\alpha)$ reads

$$N(\alpha)\sim 2\,\mathcal{I}^{(\mathrm{nos})}_{\mathrm{N}<,m=0}$$

$$\sim\frac{4}{\pi\sqrt{1+\overline{\alpha}}}\left[2\Pi_1(1,\kappa)-\frac{\mathbf{K}(\kappa)-\overline{\alpha}\mathbf{E}(\kappa)}{1-\overline{\alpha}}\right],\quad \alpha\leqslant \mathrm{O}(ka). \tag{5.17}$$

See Fig. 8 for a comparison of this expression with the exact series (2.23).

It is noted in passing that with $\kappa'=\sqrt{1-\kappa^2}$, the expansions (4.30), (4.31), and

$$\mathbf{K}(\kappa)=\ln\frac{4}{\kappa'}+\frac{1}{4}\left(\ln\frac{4}{\kappa'}-1\right)\kappa'^2+\frac{9}{64}\left(\ln\frac{4}{\kappa'}-\frac{7}{6}\right)\kappa'^4+\mathrm{O}\left(\kappa'^6\ln\frac{1}{\kappa'}\right),\quad \kappa'\to 0^+, \tag{5.18}$$

reproduce all three terms of expansion (5.4).

C. Considerations for $\alpha > O(ka)$

By following the steps of Sec. IV C, one gets

$$\mathcal{I}_{N>,m=0}(\alpha) \sim I_N(\alpha), \tag{5.19}$$

where

$$\begin{aligned} I_N(\alpha) &= \frac{ka}{\alpha}\int_1^\infty \frac{d\eta}{\sqrt{\eta^2-1}}\,\frac{e^{2ka[\Lambda-\Phi(\eta)]}}{\{1+(\eta^2-1)^{-1/2}e^{2ka[\Lambda-\Phi(\eta)]}\}^2} \\ &= \frac{1}{2\alpha}\,\eta'(\Lambda)+\frac{1}{4\alpha ka}\int_0^\infty dt\left[\eta''\left(\Lambda+\frac{t}{2ka}\right)-\eta''\left(\Lambda-\frac{t}{2ka}\right)\right]\frac{1}{1+e^t} \\ &\sim \frac{1}{2\alpha}\,\eta'(\Lambda)+\frac{\pi^2}{48\alpha(ka)^2}\,\eta'''(\Lambda), \quad ka\gg 1, \quad ka\Lambda\gg 1. \end{aligned} \tag{5.20}$$

$\Phi(\eta)$ and Λ are given by Eqs. (4.35) and (4.36). With the variable ς of Eq. (4.37),

$$\eta'(\varsigma)=\left\{\ln[\,\eta(\varsigma)+\sqrt{\eta(\varsigma)^2-1}\,]+\frac{1}{2ka}\,\frac{\eta(\varsigma)}{\eta(\varsigma)^2-1}\right\}^{-1}. \tag{5.21}$$

1. $\Lambda \gg 1$

From Eq. (5.21),

$$\eta'(\Lambda) \sim \frac{1}{\ln[\,\eta(\Lambda)+\sqrt{\eta(\Lambda)^2-1}\,]} \tag{5.22}$$

$$\sim \frac{1}{\ln[2\,\eta_0(\Lambda)]}, \tag{5.23}$$

where $\eta_0(\varsigma)$ is defined by Eq. (4.42). Furthermore,

$$\eta_0'''(\Lambda)=O[\Lambda^{-2}(\ln\Lambda)^{-2}], \quad \Lambda\to\infty. \tag{5.24}$$

It is evident that

$$I_N(\alpha)\sim\frac{1}{2\alpha}\,\eta'(\Lambda)\sim\frac{1}{2\alpha}\,\eta_0'(\Lambda), \tag{5.25}$$

with recourse to expansion (4.45). Of particular interest is the asymptotic formula

$$\mathcal{I}_{N>,m=0}(\alpha)=\frac{1}{2\alpha}\,\frac{1}{\ln\ln\alpha}\left\{1+\frac{\ln\ln\ln\alpha}{\ln\ln\alpha}+O\left[\left(\frac{\ln\ln\ln\alpha}{\ln\ln\alpha}\right)^2\right]\right\} \quad \text{as} \quad \alpha\to\infty. \tag{5.26}$$

2. $\Lambda = O(1)$

Obviously,

$$I_N(\alpha)\sim\frac{1}{2\alpha}\,\eta'(\Lambda). \tag{5.27}$$

$\eta'(\Lambda)$ is given by formula (5.22), in combination with approximation (4.51).

3. $1 \ll ka\Lambda \ll ka$

For $(ka)^{2/5} \ll ka\Lambda \ll ka$, the term proportional to $(ka)^{-1}$ in Eq. (5.21) can be neglected:

$$I_{\mathrm{N}}(\alpha) \sim \frac{1}{2\alpha}\,\eta'(\Lambda) \sim \frac{1}{2\alpha}(3\Lambda)^{-1/3}. \tag{5.28}$$

If $1 \ll ka\Lambda \ll (ka)^{2/5}$, both terms in Eq. (5.23) need to be retained. From Eq. (4.53),

$$\begin{aligned}\eta'(\Lambda) &\sim \left(\frac{ka}{2}\right)^{1/3} \frac{1}{\xi(\Lambda)^{1/2} + [4\xi(\Lambda)]^{-1}} \\ &\sim \left(\frac{ka}{2}\right)^{1/3} \tilde{\Lambda}^{-1/3}\left[1 + \frac{1}{12}\,\frac{\ln\tilde{\Lambda}}{\tilde{\Lambda}} - \frac{1}{4\tilde{\Lambda}} + \frac{1}{72}\,\frac{(\ln\tilde{\Lambda})^2}{\tilde{\Lambda}^2} - \frac{5}{48}\,\frac{\ln\tilde{\Lambda}}{\tilde{\Lambda}^2}\right].\end{aligned} \tag{5.29}$$

It is now a trivial matter to write down an expansion for $I_{\mathrm{N}}(\alpha)$.

D. Asymptotic formula for $N(\alpha)$

The foregoing discussion suggests that $\mathcal{I}^{(\mathrm{nos})}_{\mathrm{N}<,m=0}(\alpha)$ becomes of the same order of magnitude as $\mathcal{I}_{\mathrm{N}>,m=0}(\alpha)$ when $\alpha = \mathrm{O}[(ka)^{7/3}(\ln ka)^{2/3}]$. This entails that $0 < ka\Lambda = \mathrm{O}(\ln ka)$. The leading term for $N(\alpha)$ to all orders in α is

$$N(\alpha) \sim \frac{4}{\pi\sqrt{1+\overline{\alpha}}}\left[2\Pi_1(1,\kappa) - \frac{\mathbf{K}(\kappa) - \overline{\alpha}\mathbf{E}(\kappa)}{1-\overline{\alpha}}\right] + \frac{1}{\alpha}\,\eta'(\Lambda), \tag{5.30}$$

where $\overline{\alpha}$ and κ are defined by Eqs. (4.18) and (4.23), and the derivative $\eta'(\Lambda)$ is evaluated from Eq. (5.21) with (4.37).

VI. TOTAL POWER $T(\alpha)$

Despite the equality

$$T(\alpha) = \frac{\sqrt{P(\alpha)} - N(\alpha)}{\alpha}, \tag{6.1}$$

the derivation of an asymptotic formula for $T(\alpha)$ is somewhat tricky. For instance, it is clearly not allowed to replace in Eq. (6.1) $\sqrt{P(\alpha)}$ and $N(\alpha)$ for all $\alpha \leqslant \mathrm{O}(ka)$ by expressions (4.29) and (5.17) that involve complete elliptic integrals. These terms produce an erroneous formula for $T(\alpha)$ when $\tilde{\alpha}$ becomes small.

A. $\alpha \leqslant \mathrm{O}[(ka)^{2/3}]$

From Eqs. (4.2) and (5.1),

$$T(\alpha) \sim T_0(ka) - \frac{4\tilde{\alpha}}{ka}[G_{\mathrm{P}}(\tilde{\alpha}) + G_{\mathrm{N}}(\tilde{\alpha})], \quad \tilde{\alpha} = \alpha\left(\frac{ka}{2}\right)^{-2/3}, \tag{6.2}$$

where G_{P} and G_{N} are defined by Eqs. (4.4) and (5.2), and $T_0(ka)$ corresponds to the reference case already examined in Sec. III. For present purposes, it suffices to take

$$T_0(ka) \sim \frac{\gamma + \ln(32\,ka)}{\pi^2\,ka}, \quad ka \gg 1. \tag{6.3}$$

B. $\alpha \gg (ka)^{2/3}$

By invoking the large-argument approximations of Appendix B for $G_{\mathrm{P}}(\tilde{\alpha})$ and $G_{\mathrm{N}}(\tilde{\alpha})$, and scaling α by ka inside the logarithms, the right-hand side of formula (6.2) becomes

$$T_0(ka)-\frac{4\tilde{\alpha}}{ka}[G_{\mathrm{P}}(\tilde{\alpha})+G_{\mathrm{N}}(\tilde{\alpha})]\sim\frac{3}{\pi^2}\frac{1}{ka}\ln\frac{ka}{\alpha}+\frac{6\ln(4\pi)-13}{2\pi^2 ka}, \tag{6.4}$$

provided that $\tilde{\alpha}\gg 1$ while $\overline{\alpha}\ll 1$. Both of these terms are correctly reproduced by Eq. (6.1) with formulas (4.29) and (5.17), and expansions (4.30) and (5.18). Without further ado, $T(\alpha)$ is

$$T(\alpha)\sim\frac{8}{\pi^2 ka}\frac{1}{\overline{\alpha}^2}\left[1-\frac{1}{\sqrt{1+\overline{\alpha}}}\frac{\mathbf{E}(\kappa)-\overline{\alpha}\mathbf{K}(\kappa)}{1-\overline{\alpha}}\right],\quad (ka)^{2/3}\ll\alpha\leqslant \mathrm{O}(ka). \tag{6.5}$$

$\overline{\alpha}$ and κ are defined by Eqs. (4.18) and (4.23). This formula breaks down when $\alpha=\mathrm{O}[(ka)^{2/3}]$.

For larger values of α, contributions in series (2.29) representing $T(\alpha)$ arise from terms with $m=0$ and $\nu>\mathrm{O}(ka)$. Finally, a combination of expressions (4.56) and (5.30) yields

$$T\sim\frac{2ka}{\alpha^2}\left\{1-\frac{1}{\sqrt{1+\overline{\alpha}}}\frac{\mathbf{E}(\kappa)-\overline{\alpha}\mathbf{K}(\kappa)}{1-\overline{\alpha}}+[\eta(\Lambda)-1]-\frac{1}{2ka}\eta'(\Lambda)\right\},\quad \alpha\gg(ka)^{2/3}. \tag{6.6}$$

VII. REMARKS ON *C* AND *D* OPTIMUM

It is worthwhile noting the following.

(i) As pointed out in Sec. II, the constraint C of Eq. (2.8) is intended as a measure of the efficiency of the radiating system in the xy plane. In the electromagnetic case, the efficiency should express the ratio

$$\frac{\text{dissipation (Ohmic) losses}}{\text{total radiated power}}.$$

The Ohmic losses are obtained via multiplication of $C/(ka)$ by a quantity independent of a. Thus, for a fixed given frequency ω, it is desirable to employ the ratio

$$C_e=\frac{C}{ka}. \tag{7.1}$$

(ii) It follows from Eqs. (4.2), (5.1), and (6.2) that

$$\frac{D/D_0}{C_e}=kaT_0\frac{P}{N}\sim kaT_0\sim\frac{\ln(32ka)+\gamma}{\pi^2},\quad \alpha\ll ka,\quad ka\gg 1, \tag{7.2}$$

where the subscript 0 corresponds to the reference case, while

$$C_e=C_e(\alpha)\sim\left\{\frac{\ln(32ka)+\gamma}{\pi^2}-4\tilde{\alpha}[G_{\mathrm{P}}(\tilde{\alpha})+G_{\mathrm{N}}(\tilde{\alpha})]\right\}^{-1}. \tag{7.3}$$

G_{P} and G_{N} are given by Eqs. (4.4) and (5.2). In particular,

$$C_e(\alpha)\sim\frac{\pi^2}{3}\left[\ln\frac{ka}{\alpha}+\ln(4\pi)-\frac{13}{6}\right]^{-1},\quad (ka)^{2/3}\ll\alpha\ll ka. \tag{7.4}$$

Note that for $\alpha<\mathrm{O}(ka)$, D/D_0 increases moderately above 1 at the expense of a moderate increase in the constraint C_e. The slope of D/D_0, qua function of C_e, is logarithmic in ka.

For $\alpha=\mathrm{O}(ka)$,

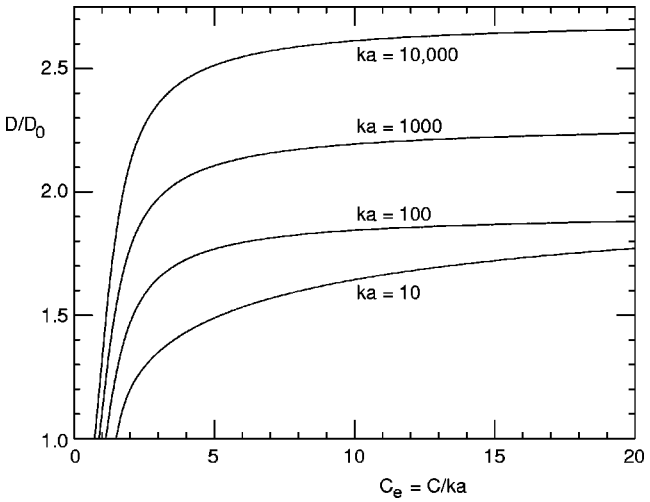

FIG. 9. Normalized directivity D/D_0 vs constraint C_e for different values of ka. D_0 is the directivity of a uniform distribution (reference case), $\alpha=0$.

$$\frac{D/D_0}{C_e}=kaT_0\mathcal{W}(\overline{\alpha}),\quad \overline{\alpha}=\frac{2\alpha}{\pi ka}=\mathrm{O}(1), \tag{7.5}$$

while C_e depends on α and ka only through $\overline{\alpha}$. In the above, $\mathcal{W}(\overline{\alpha})$ is a known function that is expressed in terms of the complete elliptic integrals (see Secs. IV and V). It follows that for fixed C_e, D/D_0 increases logarithmically in ka.

These remarks can be verified by direct comparison with Fig. 9. Notice the range of α over which D/D_0 varies almost linearly in C_e.

(iii) According to formulas (4.56), (5.30), and (6.1), if

$$ka\ll\alpha\ll(ka)^{7/3}(\ln ka)^{2/3}, \tag{7.6}$$

then

$$\sqrt{P(\alpha)}\sim\frac{2ka}{\alpha}, \tag{7.7}$$

$$T(\alpha)\sim\frac{\sqrt{P(\alpha)}}{\alpha}\sim\frac{2ka}{\alpha^2}. \tag{7.8}$$

Therefore,

$$\frac{D}{D_0}=T_0\frac{P}{T}\sim 2kaT_0\sim\frac{2}{\pi^2}[\ln(32ka)+\gamma]. \tag{7.9}$$

Evidently, this value requires an extremely large constraint C_e.

(iv) In the limit $C\to\infty$ (or $\alpha\to\infty$), expressions (4.49) and (5.26) furnish

$$C(\alpha)\sim\frac{\alpha}{\ln\alpha},\quad D(\alpha)\sim\frac{\ln\alpha}{\ln\ln\alpha}\quad\text{as}\quad\alpha\to\infty, \tag{7.10}$$

which in turn lead to

$$D \sim \frac{\ln(C \ln C)}{\ln \ln C} \quad \text{as} \quad C \to \infty. \tag{7.11}$$

Note that this formula is independent of ka and signifies Oseen's ''Einstein needle radiation.'' [19] An underlying condition when $ka \gg 1$ reads

$$\ln \frac{C}{ka} \gg ka, \tag{7.12}$$

which stems from the condition $\Lambda \gg 1$ by invoking Eq. (4.36).

VIII. OPTIMUM CURRENT $j(\phi)$

By inspection of Eq. (2.20),

$$j(\pi - \phi) = j(\phi), \quad j(-\phi) = j^*(\phi). \tag{8.1}$$

Without loss of generality, one may assume $0 \leqslant \phi \leqslant \pi/2$.

A. Remarks on the integral equation

For sufficiently small α, an approximate expression for the current can be obtained from the integral equation (2.9) according to the iterative scheme[1]

$$j^{(p)}(\phi) + \frac{\alpha}{2\pi} \int_0^{2\pi} d\phi' \, J_0\left(2ka \sin \frac{\phi - \phi'}{2}\right) j^{(p-1)}(\phi') = e^{ika \sin \phi}, \quad p = 1,2,\ldots, \tag{8.2}$$

$$j^{(0)}(\phi) = e^{ika \sin \phi}, \tag{8.3}$$

which results in a Neumann series. Evidently,

$$j(\phi) = e^{ika \sin \phi} + \sum_{p=1}^{\infty} \left(-\frac{\alpha}{ka}\right)^p \check{g}_p(\phi), \quad \alpha \ll ka, \tag{8.4}$$

where

$$\check{g}_1(\phi) = \frac{ka}{\pi} \int_0^{\pi} d\chi \, J_0(2ka \sin \chi) e^{ika \sin(\phi - 2\chi)}, \tag{8.5}$$

$$\check{g}_p(\phi) = \frac{ka}{\pi} \int_0^{\pi} d\chi \, J_0(2ka \sin \chi) \check{g}_{p-1}(\phi - 2\chi), \quad p = 2,3,\ldots. \tag{8.6}$$

When ka is large and ϕ, $\pi - \phi$ are O(1), the major contribution to integration in the preceding two equations distinctly comes from (i) neighborhoods of stationary-phase points with widths $O(1/\sqrt{ka})$, and (ii) the vicinities of $\chi = 0$, π with widths $O(1/ka)$. The stationary-phase points are given by

$$\frac{d}{d\chi}[\pm 2 \sin \chi + \sin(\phi - 2\chi)] = 0, \quad 0 < \chi < \pi, \tag{8.7}$$

or

$$\chi = \phi, \frac{\phi + n\pi}{3}, \quad n = 0,1,2. \tag{8.8}$$

The widths of the contributing regions are of the order of $(ka\sin\phi)^{-1/2}$ and $\{ka|\sin[(\phi+n\pi)/3]|\}^{-1/2}$, respectively. The total stationary-phase contribution to $\breve{g}_1(\phi)$ is

$$\breve{g}_1^{(\mathrm{sp})}(\phi)\sim\frac{1}{2\pi}\left\{\frac{e^{ika\sin\phi}}{|\sin\phi|}+\frac{1}{\sqrt{3}}\left[\frac{e^{i3ka\sin(\phi/3)-i\pi/2}}{|\sin(\phi/3)|}+\frac{e^{i3ka\sin[(\phi+2\pi)/3]-i\pi/2}}{|\sin[(\phi+2\pi)/3]|}+\frac{e^{i3ka\sin[(\phi-2\pi)/3]+i\pi/2}}{|\sin[(\phi-2\pi)/3]|}\right]\right\}, \tag{8.9}$$

while the total contribution from the end points $\chi=0,\pi$ is

$$\breve{g}_1^{(\mathrm{ep})}(\phi)\sim\frac{2ka}{\pi}\int_0^\infty d\chi\,J_0(2ka\chi)e^{ika\sin\phi-i2ka\chi\cos\phi}=\frac{e^{ika\sin\phi}}{\pi|\sin\phi|}. \tag{8.10}$$

Therefore, to the lowest order in $(ka)^{-1}$,

$$\breve{g}_1(\phi)\sim\frac{3}{2\pi}\frac{e^{ika\sin\phi}}{|\sin\phi|}+\frac{1}{2\pi\sqrt{3}}\left\{\frac{e^{i3ka\sin(\phi/3)-i\pi/2}}{|\sin(\phi/3)|}+\frac{e^{i3ka\sin[(\phi+2\pi)/3]-i\pi/2}}{|\sin[(\phi+2\pi)/3]|}+\frac{e^{i3ka\sin[(\phi-2\pi)/3]+i\pi/2}}{|\sin[(\phi-2\pi)/3]|}\right\}. \tag{8.11}$$

The preceding calculations can be extended to higher orders in α, but the iteration procedure becomes increasingly cumbersome. In view of Eq. (8.6), the pth iteration ($p\geqslant 2$) introduces stationary-phase points that solve

$$\frac{d}{d\chi}\left[\pm 2\sin\chi+(2p-1)\sin\left(\frac{\phi-2\chi+2n\pi}{2p-1}\right)\right]=0,\quad n=-(p-1),\ldots,p-1. \tag{8.12}$$

These points are

$$\chi_n=\begin{cases}\dfrac{\phi+(2n+2p-1)\pi}{2p+1}, & n=-(p-1),\ldots,-1,0\\[2ex] \dfrac{\phi+2n\pi}{2p+1}, & n=0,1,\ldots,p-1\\[2ex] \dfrac{\phi+2(n+2p-1)\pi}{2p+1}, & n=-p+1,\end{cases} \tag{8.13}$$

with corresponding phases

$$(2p+1)ka\sin\psi_{pm},\quad m=-p,-p+1,\ldots,p-1,p, \tag{8.14}$$

where

$$\psi_{pm}=\frac{\phi+2m\pi}{2p+1},\quad m=-p,-p+1,\ldots,p-1,p. \tag{8.15}$$

For non-negative m which is less than or equal to $p/2$, ψ_{pm} represents the reflection angle $\overline{\psi}_{pm}$ at the local tangent of a ray that originates from the x axis, travels in the direction of maximum field at $\phi=\pi/2$, and reaches the observation point after bouncing p times at the circular boundary counterclockwise, with m being the winding number. For larger values of m, $\pi-\psi_{pm}$ becomes the reflection angle, the sense of circulation is clockwise, and $p-m$ is the winding number. When

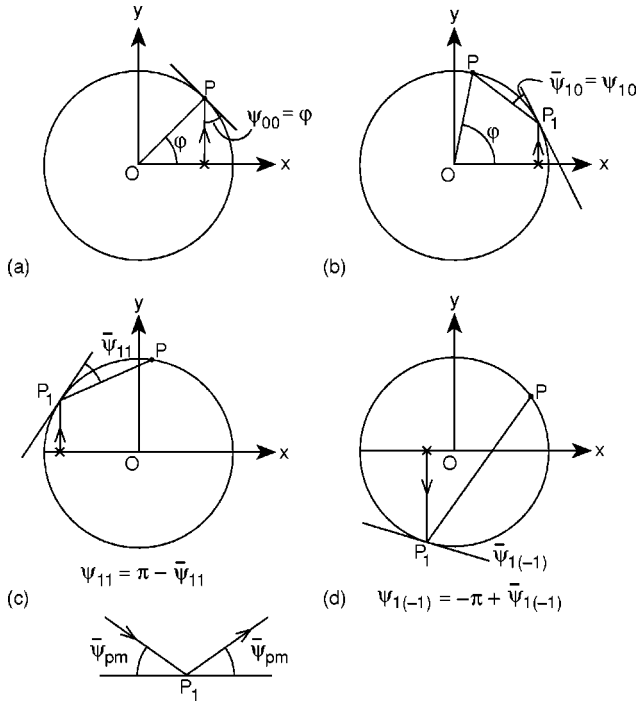

FIG. 10. A geometric interpretation of iterative formula (8.2) with ψ_{pm} from Eq. (8.15) and $p=0,1$. P is the observation point and P_1 the point at reflection. (a) $p=0$, $m=0\,(+)$, (b) $p=1$, $m=0\,(+)$, (c) $p=1$, $m=1\,(+)$, (d) $p=1$, $m=-1\,(-)$.

m is negative, the ray runs initially antiparallel to the positive y axis and the previous considerations hold with m being replaced by $|m|$ and ψ_{pm} by $-\psi_{pm}$, and the sense of circulation reversed in each case. See Figs. 10(a)–10(d), for $p=0,1$, and Figs. 11(a)–11(e) for $p=2$.

Because the expansion parameter here is proportional to $\alpha/(ka)$, this scheme is restricted in its applicability. Furthermore, when $\phi=\mathrm{O}[(ka)^{-1/3}]$, $\chi=0$ falls inside the critical region of the stationary-phase points at $\chi=\phi/(2p+1)$ $(p=0,1,2,\ldots)$ and the approximations made hitherto break down. This case is particularly interesting because the major contribution to the maximum field at $\phi=\pi/2$ is determined by the current in the vicinities of $\phi=0,\pi$. Indeed, in view of Eqs. (2.4) and (8.4), consider the integral

$$\int_0^{2\pi} d\phi'\, e^{-ika\cos(\phi-\phi')} e^{i(2p+1)ka\sin[(\phi'+2m\pi)/(2p+1)]}. \tag{8.16}$$

With $\phi=\pi/2+\epsilon$, $|\epsilon|\ll 1$, stationary-phase points are located at

$$\phi'=\left(1+\frac{1}{2p}\right)\left(\epsilon+\frac{2m\pi}{2p+1}\right), \quad m=0,1,2,\ldots, \quad p=1,2,\ldots. \tag{8.17}$$

For $m=0$, these points fall arbitrarily close to 0.

B. Asymptotic expansion for $j(\phi)$, $\phi=\mathrm{O}(1)$, $\pi-\phi=\mathrm{O}(1)$

To get an asymptotic expansion for $j(\phi)$, start with Eqs. (2.26) and (2.34), and

$$\frac{1}{1-(\tau_1 A)^2}=\sum_{p=0}^{L-1}(\tau_1 A)^{2p}+\frac{(\tau_1 A)^{2L}}{1-(\tau_1 A)^2}, \quad |\tau_1(\nu)A(\nu)|<1, \quad \nu\text{: positive}, \tag{8.18}$$

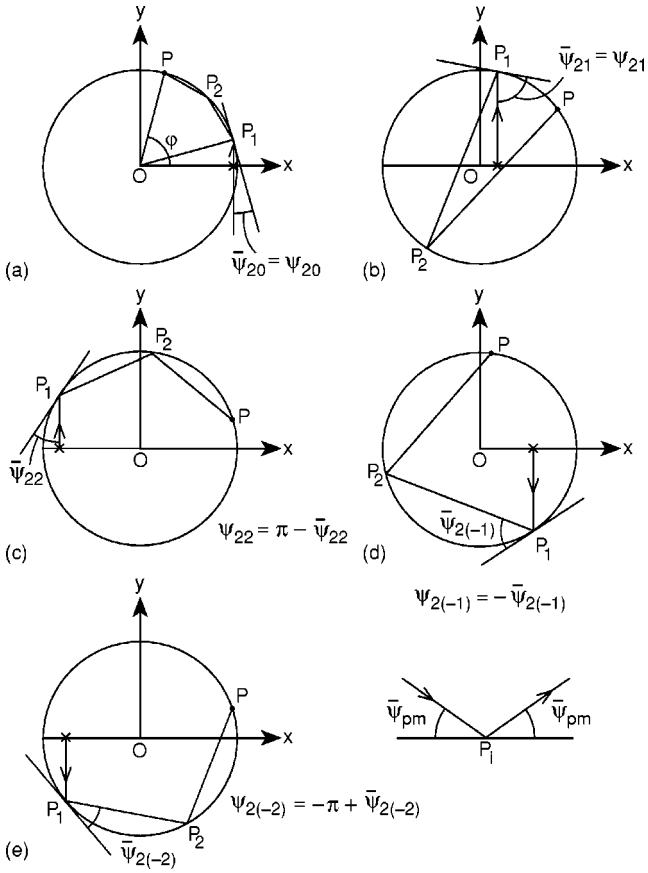

FIG. 11. A geometric interpretation of formula (8.2) with (8.14) and ψ_{pm} from Eq. (8.15), and $p=2$. P is the observation point and P_i, $i=1,2$, points at reflection. (a) $m=0\,(+)$, (b) $m=1\,(+)$, (c) $m=2\,(+)$, (d) $m=-1\,(-)$, (e) $m=-2\,(-)$.

along with its complex conjugate involving $B=B(\nu)$. In the limit $L\to\infty$,

$$j(\phi)=\sum_{p=0}^{\infty}\sum_{m=-\infty}^{\infty}[\check{J}_{pm}(\phi)+\check{J}_{pm}(\pi-\phi)]. \tag{8.19}$$

A rigorous justification of this expansion is a trifling matter. In the above,

$$\check{J}_{pm}(\phi)=\int_0^{\infty}\frac{d\nu}{\tau_2(\nu)^2+\alpha A(\nu)B(\nu)}[A(\nu)(\tau_1 A)^{2p}+B(\nu)(\tau_1 B)^{2p}]e^{i\nu(\phi+2m\pi)}. \tag{8.20}$$

These integrals can be evaluated by the standard method of stationary phase. The associated overall phase reads

$$\mathcal{P}_{pm\pm}(\nu;\phi)=\pm(2p+1)\sqrt{(ka)^2-\nu^2}\mp(2p+1)\,\nu\arccos[\nu/(ka)]\mp(2p+1)\frac{\pi}{4}+\nu\phi+2m\pi\nu. \tag{8.21}$$

In the first branch of arccos, $\mathcal{P}_{pm\pm}(\nu>0;\phi)$ is rendered stationary at

$$\nu_{pm\pm}^{(\mathrm{sp})}=ka\cos\psi_{pm}, \tag{8.22a}$$

where

$$+:\ 0<\psi_{pm}\leqslant\pi/2,\quad -:\ -\pi/2\leqslant\psi_{pm}<0, \tag{8.22b}$$

and ψ_{pm} is defined by Eq. (8.15), while

$$\mathcal{P}^{(\mathrm{sp})}_{pm\pm}=(2p+1)ka\sin\psi_{pm}\mp(2p+1)\frac{\pi}{4},\quad \left.\frac{d^2\mathcal{P}_{pm\pm}}{d\nu^2}\right|_{\nu=\nu^{(\mathrm{sp})}_{pm\pm}}=\pm\frac{2p+1}{ka\sin\psi_{pm}}. \tag{8.23}$$

Condition (8.22b) poses a restriction on the allowed values of m for fixed p:

$$\begin{aligned}+:&\ \begin{cases}0\leqslant 2m\leqslant p, & 0<\phi\leqslant\pi/2\\ 0\leqslant 2m\leqslant p-1, & \pi/2<\phi<\pi,\end{cases}\\ -:&\ \begin{cases}-p\leqslant 2m\leqslant -1, & 0<\phi\leqslant\pi/2\\ -p-1\leqslant 2m\leqslant -1, & \pi/2<\phi<\pi.\end{cases}\end{aligned} \tag{8.24}$$

Consequently,

$$\begin{aligned}\check{J}_{pm}(\phi)\sim 2\frac{(-\overline{\alpha})^p}{\sqrt{2p+1}}&\frac{1}{[|\sin\psi_{pm}|^{1/2}+\sqrt{|\sin\psi_{pm}|+\overline{\alpha}}]^{2p+1}}\frac{|\sin\psi_{pm}|}{\sqrt{|\sin\psi_{pm}|+\overline{\alpha}}}\\ &\times\exp[i(2p+1)ka\sin\psi_{pm}-ip\pi/2],\quad 0\leqslant 2m\leqslant p,\end{aligned} \tag{8.25}$$

or

$$\begin{aligned}\check{J}_{pm}(\phi)\sim 2\frac{(-\overline{\alpha})^p}{\sqrt{2p+1}}&\frac{1}{[|\sin\psi_{pm}|^{1/2}+\sqrt{|\sin\psi_{pm}|+\overline{\alpha}}]^{2p+1}}\frac{|\sin\psi_{pm}|}{\sqrt{|\sin\psi_{pm}|+\overline{\alpha}}}\\ &\times\exp[i(2p+1)ka\sin\psi_{pm}+ip\pi/2],\quad -p\leqslant 2m\leqslant -1,\end{aligned} \tag{8.26}$$

where $\overline{\alpha}$ is given by Eq. (4.18). It follows from Eq. (8.19) that

$$\begin{aligned}j(\phi)\sim 2\sum_{p=0}^{\infty}\frac{(-\overline{\alpha})^p}{\sqrt{2p+1}}&\sum_{s=\pm}\sum_{m\in S_{ps}}\frac{1}{[|\sin\psi_{pm}|^{1/2}+\sqrt{|\sin\psi_{pm}|+\overline{\alpha}}]^{2p+1}}\\ &\times\frac{|\sin\psi_{pm}|}{\sqrt{|\sin\psi_{pm}|+\overline{\alpha}}}\exp[i(2p+1)ka\sin\psi_{pm}-isp\pi/2],\end{aligned} \tag{8.27}$$

$$S_{p+}=\{\text{integer } m:\ 0\leqslant m\leqslant p\},\quad S_{p-}=\{\text{integer } m:\ -p\leqslant m\leqslant -1\}. \tag{8.28}$$

The condition $0<|\psi_{pm}|\leqslant\pi/2$ is now replaced by $0<|\psi_{pm}|<\pi$.

This ray representation for the optimum current is reminiscent of the geometrical optics for electromagnetic fields. With $p\gg 1$ and fixed m and $\overline{\alpha}$, each corresponding term of the series is of the order of $p^{-3/2}$ and absolute convergence obtains. For $\alpha<\pi ka\min_{pm}|\sin\psi_{pm}|/2$, the summands can be expanded in powers of $\overline{\alpha}$. Note that[16]

$$(1+\sqrt{1+z})^{-2p-1}=2^{-2p-1}{}_2F_1(p+\tfrac{1}{2},p+1;2p+2;-z), \tag{8.29}$$

where ${}_2F_1$ is the hypergeometric function and $z=\overline{\alpha}|\sin\psi_{pm}|^{-1}$. Expanding ${}_2F_1$ readily reproduces asymptotic formulas for the iterative solutions described by Eqs. (8.2)–(8.6).

Investigating expansion (8.27) in routine mathematical rigor is beyond the scope of this paper. A condition for its validity is

$$\alpha\leqslant\mathrm{O}(ka), \tag{8.30}$$

while expansions (8.25) and (8.26) make sense if

$$|\psi_{pm}|,\ |\pi-\psi_{pm}|>\mathrm{O}[(ka)^{-1/3}], \tag{8.31}$$

at least for $p,\ m\leqslant \mathrm{O}(1)$. The latter conditions follow from the requirement that the stationary-phase points lie outside the transitional region of the Bessel functions. For $p=\mathrm{O}(1)$, the first one of conditions (8.31) is violated when $m=0$ and $\phi=\mathrm{O}[(ka)^{-1/3}]$.[20]

In the next paragraphs, attention focuses on the ranges $\alpha\leqslant \mathrm{O}(ka)$ and $0\leqslant\phi\leqslant \mathrm{O}[(ka)^{-1/3}]$. From a practical viewpoint, this case is perhaps the most interesting one, since it amounts to an optimum directivity D that is moderately larger than the directivity D_0 of the uniform distribution.

C. Case $0\leqslant\phi\leqslant \mathrm{O}[(ka)^{-1/3}]$, $\alpha\leqslant \mathrm{O}(ka)$

Consider $\alpha\leqslant \mathrm{O}[(ka)^{2/3}]$. The optimum current is approximated by[17,18]

$$\begin{aligned} j(\phi)&\sim \int_0^\infty d\nu\,\frac{J_\nu(ka)}{1+\alpha J_\nu(ka)^2}\,e^{i\nu\phi}\\ &\sim e^{ika\phi}\int_{-\infty}^{\infty} d\xi\,\frac{\mathrm{Ai}(\xi)}{1+\tilde{\alpha}\,\mathrm{Ai}(\xi)^2}\,e^{i\tilde{\phi}\xi},\quad \tilde{\alpha}=\alpha\left(\frac{ka}{2}\right)^{-2/3}\leqslant \mathrm{O}(1), \end{aligned} \tag{8.32}$$

where

$$\tilde{\phi}=\phi\left(\frac{ka}{2}\right)^{1/3}\leqslant \mathrm{O}(1). \tag{8.33}$$

It has not been possible to evaluate the requisite integral in terms of known transcendental functions when $\tilde{\phi}=\mathrm{O}(1)$ and $\tilde{\alpha}=\mathrm{O}(1)$.

By virtue of Eq. (C31) of Appendix C,

$$\begin{aligned} j(\phi)&\sim e^{ika\phi}\left[\int_{-\infty}^{\infty} d\xi\,\mathrm{Ai}(\xi)e^{i\tilde{\phi}\xi}-\tilde{\alpha}\int_{-\infty}^{\infty} d\xi\,\mathrm{Ai}(\xi)^3 e^{i\tilde{\phi}\xi}\right]\\ &=e^{ika(\phi-\phi^3/6)}-\tilde{\alpha}\tilde{\phi}^{1/2}\frac{e^{-i\pi/6}}{3\sqrt{2\pi}}\left[J_{1/6}\left(\frac{2}{27}ka\phi^3\right)\right.\\ &\quad\left.+\frac{1}{2}e^{-i\pi/3}H^{(2)}_{1/6}\left(\frac{2}{27}ka\phi^3\right)\right]e^{ika(\phi-5\phi^3/54)},\\ &\tilde{\alpha}\ll 1,\ ka\phi^5\ll 1. \end{aligned} \tag{8.34}$$

This result agrees with expression (8.27) when $\tilde{\phi}\gg 1$. Indeed, the substitutions

$$J_{1/6}\left(\frac{2}{27}ka\phi^3\right)\sim\frac{3\sqrt{3}}{\sqrt{\pi ka\phi^3}}\cos\left(\frac{2}{27}ka\phi^3-\frac{\pi}{3}\right),$$

$$H^{(2)}_{1/6}\left(\frac{2}{27}ka\phi^3\right)\sim\frac{3\sqrt{3}}{\sqrt{\pi ka\phi^3}}\,e^{-i(2ka\phi^3/27-\pi/3)}$$

into formula (8.34) for $\phi\gg(ka)^{-1/3}$ and $\alpha\ll(ka)^{2/3}$ give

$$j(\phi)\sim\left(1-\frac{3\alpha}{2\pi ka\phi}\right)e^{ika(\phi-\phi^3/6)}-\frac{\sqrt{3}\alpha}{2\pi ka\phi}\,e^{ika(\phi-\phi^3/54)-i\pi/2}. \tag{8.35}$$

On the other hand,

$$2\sum_{p=0}^{\infty}\frac{(-\overline{\alpha})^p}{\sqrt{2p+1}}\frac{1}{[|\sin\psi_{p0}|^{1/2}+\sqrt{|\sin\psi_{p0}|+\overline{\alpha}}]^{2p+1}}\frac{|\sin\psi_{p0}|}{\sqrt{|\sin\psi_{p0}|+\overline{\alpha}}}e^{i(2p+1)ka\sin\psi_{p0}-ip\pi/2}$$

$$\sim 2\left[\frac{1}{\sqrt{\sin\phi+\sqrt{\sin\phi+\overline{\alpha}}}}\frac{\sin\phi}{\sqrt{\sin\phi+\overline{\alpha}}}e^{ika\sin\phi}\right.$$

$$\left.-\frac{\overline{\alpha}}{\sqrt{3}}\frac{1}{[\sqrt{\sin(\phi/3)}+\sqrt{\sin(\phi/3)+\overline{\alpha}}]^3}\frac{\sin(\phi/3)}{\sqrt{\sin(\phi/3)+\overline{\alpha}}}e^{i3ka\sin(\phi/3)-i\pi/2}\right]. \tag{8.36}$$

With the approximations

$$\frac{1}{\sqrt{\phi}+\sqrt{\phi+\overline{\alpha}}}\sim\frac{1}{2\sqrt{\phi}}\left(1-\frac{\overline{\alpha}}{4\phi}\right),\quad \frac{1}{\sqrt{\phi+\overline{\alpha}}}\sim\frac{1}{\sqrt{\phi}}\left(1-\frac{\overline{\alpha}}{2\phi}\right),$$

$$\frac{1}{[\sqrt{\phi/3}+\sqrt{\phi/3+\overline{\alpha}}]^3}\sim\frac{3\sqrt{3}}{8\phi^{3/2}},\quad \alpha\ll ka\phi,$$

the sum (8.36) reduces to

$$j(\phi)\sim\left(1-\frac{3\alpha}{2\pi ka\phi}\right)e^{ika\sin\phi}-\frac{\sqrt{3}\alpha}{2\pi ka\phi}e^{i3ka\sin(\phi/3)-i\pi/2}. \tag{8.37}$$

Obviously, expression (8.35) is recovered if $\phi\ll(ka)^{-1/5}$.

With $\tilde{\alpha}=\mathrm{O}(1)$ and $\tilde{\phi}\gg 1$, the major contribution to the integral (8.32) stems from stationary-phase points that are distributed along the negative ξ axis. These are singled out by expanding the integrand according to Eq. (8.18),

$$\frac{\mathrm{Ai}(\xi)}{1+\tilde{\alpha}\,\mathrm{Ai}(\xi)^2}=\frac{1}{\tau_2^2+\tilde{\alpha}AB}\left\{\sum_{p=0}^{L-1}[(\tau_1A)^{2p}A+(\tau_1B)^{2p}B]+\frac{(\tau_1A)^{2L}A}{1-(\tau_1A)^2}+\frac{(\tau_1B)^{2L}B}{1-(\tau_1B)^2}\right\}, \tag{8.38}$$

where

$$A=A(\xi)=e^{-i\pi/3}\mathrm{Ai}(|\xi|e^{-i\pi/3}),\quad B=B(\xi)=e^{i\pi/3}\mathrm{Ai}(|\xi|e^{i\pi/3}), \tag{8.39}$$

$\tau_1=\tau_1(\xi)$ and $\tau_2=\tau_2(\xi)$ are given by Eq. (2.33) with α being replaced by $\tilde{\alpha}$, and $1\ll L=\mathrm{O}(\tilde{\phi})$ so that the remainders when L terms are summed can be neglected. Take $L\to\infty$ once the stationary-phase calculation is carried out. Notably, the stationary-phase points lie away from the origin and large-argument approximations for the Airy functions become effective. The ensuing expansion connects smoothly to the $m=0$ terms of series (8.27) with

$$\sin\psi_{p0}\sim\frac{\phi}{2p+1}$$

in the amplitude, and

$$\sin\psi_{p0}\sim\frac{\phi}{2p+1}-\frac{1}{6}\frac{\phi^3}{(2p+1)^3},\quad \frac{ka\phi^5}{(2p+1)^5}\ll 1,$$

in the phase.

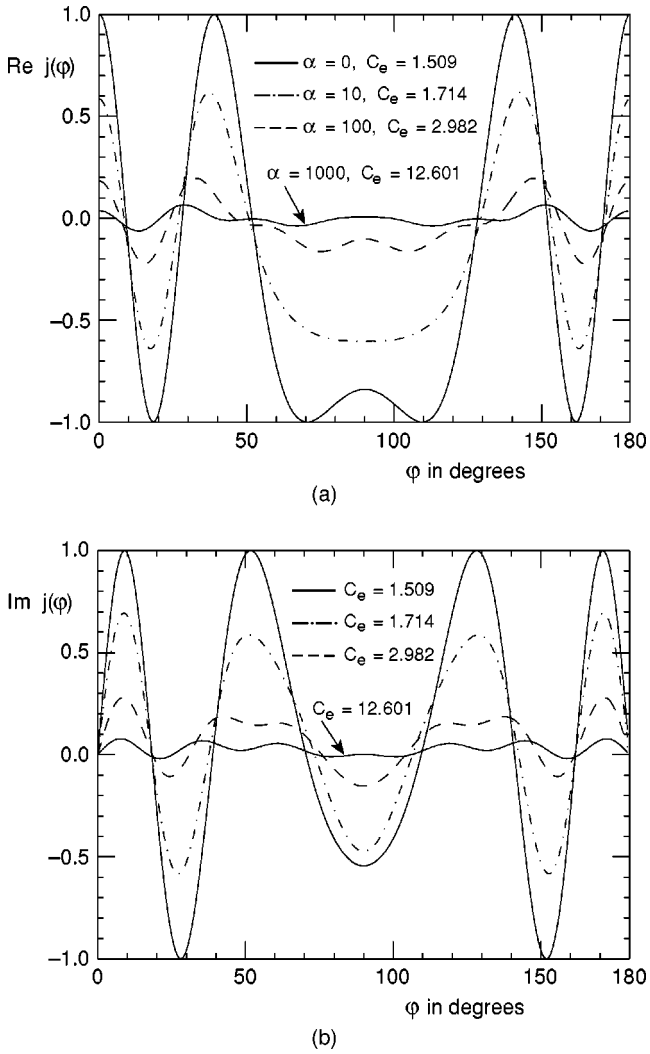

FIG. 12. (a) Real part of the optimum current $j(\varphi)$ from exact series (2.20) for $ka=10$ and different values of the constraint C_e. (b) Imaginary part of the optimum current $j(\varphi)$ from exact series (2.20) for $ka=10$.

The case $\alpha > \mathrm{O}[(ka)^{2/3}]$ is more involved, because contributions to the integral (8.32) arise from positive ξ such that $\tilde{\alpha}\,\mathrm{Ai}(\xi)^2 = \mathrm{O}(1)$, in addition to the $m \neq 0$ terms from series (8.27). When $\tilde{\phi} \leqslant \mathrm{O}(1)$ and $\overline{\alpha} = \mathrm{O}(1)$, the former contributions may become negligible.

D. Graphical representations of $j(\phi)$ and far-field pattern

In Figs. 12(a) and 12(b), the real and imaginary parts of the optimum current $j(\phi)$ are plotted versus ϕ $(0 \leqslant \phi \leqslant \pi)$ for four different values of the constraint C_e. The corresponding radiation patterns scaled as $|\psi(\hat{\mathbf{r}})|/\psi(\hat{\mathbf{y}})$ are shown in Fig. 13. As expected intuitively, the number of the side lobes increases while their size decreases with C_e.

IX. CONCLUSIONS AND DISCUSSION

Starting with a familiar boundary-value problem for the wave equation, this paper applies the general scheme of Ref. 1 in order to analyze optimally directive circular currents in two space dimensions. The integral equation for the current is solved exactly in terms of Fourier series and the optimal quantities, such as the directivity, are evaluated approximately for large values of the

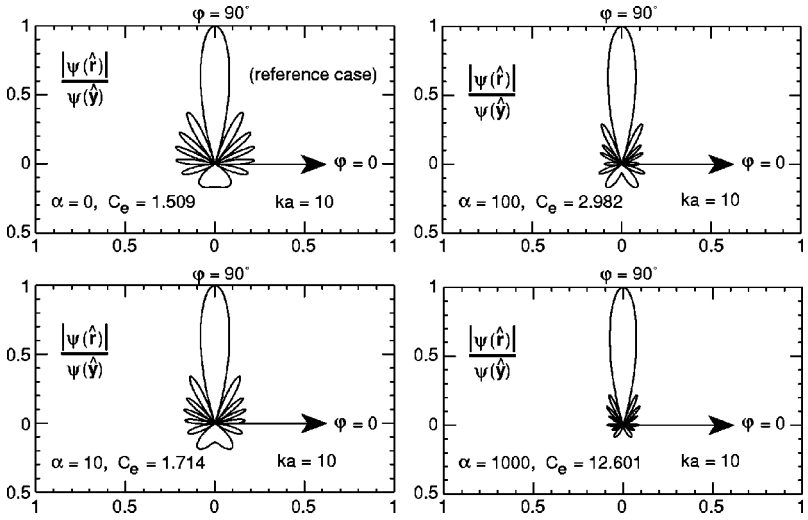

FIG. 13. Normalized optimum radiation pattern from exact series (2.21) for $ka=10$.

electrical radius ka. A noteworthy indication of this study is that large radiating structures can be advantageous for the achievement of directivities moderately larger than the directivity D_0 of the uniform current distribution. In the case of the circle, a more precise statement quantified in Sec. VII is that the rate of the directivity increase slightly above D_0 is logarithmic in ka. Intuitively, a similar result is expected to hold for some class of sufficiently smooth and convex closed loops of electrically large linear dimensions.

The asymptotic analysis reveals oscillatory optimum currents that can be represented by geometrical rays bouncing and circulating inside the circle. This picture breaks down in the vicinity of width $\mathrm{O}[(ka)^{-1/3}]$ of points (a,ϕ) which contribute to the leading order in the maximum of the radiation field, and lie in a direction perpendicular to that of the maximum peak. A formula to remedy this anomaly has been provided for directivities moderately larger than D_0. It is expected that a somewhat analogous picture should hold for a wide class of convex, simple closed curves $\mathcal{C}$, where the specifics of the ray structure depend on the radius of curvature $r_c(s)$.[21] The principal contribution to the field in the direction of maximum may then be determined from the behavior of the current in the vicinities of the local extrema of $r_c(s)$.

As implied by Oseen's analysis,[19] the Einstein needle radiation requires optimal currents reversing extremely rapidly along the loop, with large values of the constraint C $(\alpha\to\infty)$. Then the normalized far-field pattern tends to resemble a needle in the direction of maximum directivity. For $\alpha\to\infty$ and $ka\geqslant \mathrm{O}(1)$, the Fourier series (2.20) for the current can be reasonably approximated by noticing that the major contribution to summation comes from all integer n's for which condition (4.16) is satisfied (with ν replaced by n). Thus, there is always a contributing region that lies above the transition point ka; there, the Bessel functions decrease exponentially in n. As expected, the corresponding terms exhibit rapid oscillations in ϕ. In addition, there is possibly another contributing region, $n<ka$, where the Bessel functions have zeros qua functions of their index. For certain narrow ranges of ka, some of these zeros may happen to fall sufficiently close to integers and the corresponding terms have a magnitude of the order of $1/\sqrt{\alpha}$. This rather exceptional case is not investigated any further in this paper.

The leading term of an asymptotic expansion for the directivity D as $C\to\infty$ is intimately related to the behavior as $m\to\infty$ of the logarithms $\ln|\alpha_m|$, where a_m are the eigenvalues pertaining to integral equation (2.9). Under quite restrictive conditions on the convexity and smoothness of $\mathcal{C}$, it can be conjectured that this leading behavior approximates, in some sense, the one for $\alpha_m = -J_m(ka)^{-2}$. It is therefore expected that there exists a class of curves $\mathcal{C}$ that reasonably satisfy the asymptotic formula (7.11). The required consistency conditions such as the degree of smoothness of $\mathcal{C}$ are left as an open question for future research.

A next step is to extend the methodology applied hitherto to the cases of circular and noncircular loops embedded in a three-dimensional space. An intriguing question that could be addressed is whether the optimum current examined in this paper may resemble, and if so in what sense, a current that can be excited on resonant, noncircular closed-loop arrays of cylindrical dipoles.[5] If the answer to this question is positive, it may be possible to excite the optimum current distributions in convex, noncircular loops.

ACKNOWLEDGMENTS

The authors are greatly indebted to Professor Tai Tsun Wu for his suggestion of the problem and his constant encouragement. Without his advice this paper could not have been written. They are also grateful to Professor Ronold W. P. King for various useful discussions. Special thanks are due to Dr. John Myers for valuable suggestions, and to Margaret Owens for her assistance throughout the preparation of the manuscript. D.M. wishes to thank Professor Nicola Khuri for his hospitality at The Rockefeller University. Under G.F.'s present affiliation, his work was supported by the Greek Secretariat of Research and Technology; under his former affiliation with AFRL/SN, Hanscom AFB, MA, his work was supported by AFOSR under Project No. 2304IN01.

APPENDIX A: ON THE POISSON SUMMATION FORMULA

By relaxing the requirements of mathematical rigor, consider the series

$$S=\sum_{n=0}^{\infty} f(n). \tag{A1}$$

When $f(n)$ is properly replaced by $f(\nu$:complex), the Poisson summation formula can be derived from the ''Watson transformation.'' [22] It is assumed that the positive real axis, including $\nu=0$, is free of any singularities of $f(\nu)$. Clearly,

$$S=\frac{-1}{2i}\oint_{\Gamma} d\nu \frac{f(\nu)}{\tan \pi\nu}, \tag{A2}$$

where the contour Γ is wrapped around the positive real axis clockwise, leaving all singularities of $f(\nu)$ outside the enclosed region. Let $\Gamma_{\pm}$ be a portion of Γ lying in the upper $(+)$ or lower $(-)$ half of the ν plane, and Γ_{ϵ} a semicircle of small (finite) radius ϵ, centered at $\nu=0$, such that $\Gamma=\Gamma_{+}\cup\Gamma_{\epsilon}\cup\Gamma_{-}$. The expansion of $(1/\tan \pi\nu)$ as

$$\frac{1}{\tan \pi\nu}=\mp i\left\{\sum_{n=0}^{N_{\pm}-1}[e^{\pm i2\pi n\nu}+e^{\pm i2\pi(n+1)\nu}]+\frac{e^{\pm i2\pi\nu N_{\pm}}(1+e^{\pm i2\pi\nu})}{1-e^{\pm i2\pi\nu}}\right\}, \quad \nu\in\Gamma_{\pm}, \tag{A3}$$

and subsequent use of the limits $N_{\pm}\to\infty$ independently while keeping ϵ fixed, furnish

$$S=\frac{1}{2}\lim_{N_{\pm}\to\infty}\left\{\sum_{n=0}^{N_{+}-1}\int_{\Gamma_{+}} d\nu f(\nu)[e^{i2\pi n\nu}+e^{i2\pi(n+1)\nu}]\right.$$
$$\left.-\sum_{n=0}^{N_{-}-1}\int_{\Gamma_{-}} d\nu f(\nu)[e^{-i2\pi n\nu}+e^{-i2\pi(n+1)\nu}]\right\}-\frac{1}{2i}\int_{\Gamma_{\epsilon}} d\nu \frac{f(\nu)}{\tan \pi\nu}. \tag{A4}$$

In the limit $\epsilon\to 0^{+}$, the integration over Γ_{ϵ} picks up half the residue of $[f(\nu)/\tan \pi\nu]$ at $\nu=0$, leading to

$$\sum_{n=0}^{\infty} f(n)=\tfrac{1}{2}f(0)+\lim_{N_{\pm}\to\infty}\sum_{n=-N_{-}}^{N_{+}}\int_{0}^{\infty} d\nu f(\nu)e^{i2\pi n\nu}. \tag{A5}$$

APPENDIX B: EVALUATION OF $G_{\mathrm{P}}(x)$ AND $G_{\mathrm{N}}(x)$ FOR $x \gg 1$

In this Appendix, the integrals $G_{\mathrm{P}}(x)$ and $G_{\mathrm{N}}(x)$ of Eqs. (4.4) and (5.2) are evaluated for $x \gg 1$ by the Mellin transform technique.

1. Integral $G_{\mathrm{P}}(x)$

The Mellin transform of $G_{\mathrm{P}}(x)$ equals

$$\overline{G}_{\mathrm{P}}(\zeta)=\int_0^\infty dx\, x^{-\zeta} G_{\mathrm{P}}(x)=\frac{\pi}{\sin \pi\zeta}\int_{-\infty}^{\infty} d\xi\,[\mathrm{Ai}(\xi)^2]^{2+\zeta}, \quad 0<\mathrm{Re}\,\zeta<1. \tag{B1}$$

The strip given here is the region where the original integral of the Mellin transform converges. The function $\overline{G}_{\mathrm{P}}(\zeta)$ may be continued analytically to the entire ζ plane.

When $\zeta \to 0^+$, the integral of Eq. (B1) tends to diverge in $-\infty$. In the spirit of Sec. III, the first two terms of the asymptotic expansion of $G_{\mathrm{P}}(x)$ as $x\to\infty$ can be determined by expanding $\overline{G}_{\mathrm{P}}(\zeta)$ in powers of ζ in the vicinity of $\zeta=0$. By writing

$$\int_{-\infty}^{\infty} d\xi\,[\mathrm{Ai}(\xi)^2]^{2+\zeta}=\int_{\delta}^{\infty} d\xi\,[\mathrm{Ai}(-\xi)^2]^{2+\zeta}+\int_{-\delta}^{\infty} d\xi\,[\mathrm{Ai}(\xi)^2]^{2+\zeta}, \quad 0<\delta=\mathrm{O}(1), \tag{B2}$$

it is recognized that only the first term becomes singular as $\zeta\to 0$. Specifically,

$$\int_{\delta}^{\infty} d\xi[\mathrm{Ai}(-\xi)^2]^{2+\zeta}\sim \pi^{-2-\zeta}\int_{\delta}^{\infty} d\xi\left[\xi^{-1/2}\sin^2\left(\frac{2}{3}\xi^{3/2}+\frac{\pi}{4}\right)\right]^{2+\zeta} + \int_{\delta}^{\infty} d\xi\left[\mathrm{Ai}(-\xi)^4-\pi^{-2}\xi^{-1}\sin^4\left(\frac{2}{3}\xi^{3/2}+\frac{\pi}{4}\right)\right]. \tag{B3}$$

While nothing further needs to be done about the second term of this formula, the first one is approximated as follows:

$$\begin{aligned}
&\pi^{-2-\zeta}\int_{\delta}^{\infty} d\xi\left[\xi^{-1/2}\sin^2\left(\frac{2}{3}\xi^{3/2}+\frac{\pi}{4}\right)\right]^{2+\zeta}\\
&\quad\sim \pi^{-2-\zeta}\int_{\delta}^{\infty} d\xi\,\xi^{-1-\zeta/2}\sin^4\left(\frac{2}{3}\xi^{3/2}+\frac{\pi}{4}\right)\left[1+\zeta\ln\sin^2\left(\frac{2}{3}\xi^{3/2}+\frac{\pi}{4}\right)\right]\\
&\quad\sim \pi^{-2-\zeta}\int_{\delta}^{\infty} d\xi\,\xi^{-1-\zeta/2}\sin^4\left(\frac{2}{3}\xi^{3/2}+\frac{\pi}{4}\right)+2\,\pi^{-2-\zeta}\langle \sin^4(\theta+\pi/4)\ln\sin^2(\theta\\
&\qquad+\pi/4)\rangle\,\delta^{-\zeta/2} \quad \text{as} \quad \zeta\to 0^+,
\end{aligned} \tag{B4}$$

where

$$\langle \sin^4(\theta+\pi/4)\ln\sin^2(\theta+\pi/4)\rangle=\frac{1}{2\pi}\int_0^{2\pi} d\theta\,\sin^4\theta\ln\sin^2\theta=-\frac{3}{4}\ln 2+\frac{7}{16}, \tag{B5}$$

$$\int_{\delta}^{\infty} d\xi\,\xi^{-1-\zeta/2}\sin^4\left(\frac{2}{3}\xi^{3/2}+\frac{\pi}{4}\right)=\int_{\delta}^{\infty} d\xi\,\xi^{-1-\zeta/2}\left[\frac{3}{8}-\frac{1}{8}\cos\left(\frac{8}{3}\xi^{3/2}\right)+\frac{1}{2}\sin\left(\frac{4}{3}\xi^{3/2}\right)\right]$$

$$\sim \frac{3}{4\zeta}\left(1-\frac{\zeta}{2}\ln\delta\right)+\int_{\delta}^{\infty}\frac{d\xi}{\xi}\left[-\frac{1}{8}\cos\left(\frac{8}{3}\xi^{3/2}\right)+\frac{1}{2}\sin\left(\frac{4}{3}\xi^{3/2}\right)\right]. \tag{B6}$$

Note that the preceding integral is canceled exactly by terms produced by the second integral in the right-hand side of approximation (B3).

The combination of formulas (B1)–(B6) yields

$$\overline{G}_{\mathrm{P}}(\zeta)\sim\frac{3}{4\pi^2\zeta^2}-\frac{Ł}{8\pi^2\zeta}\quad\text{as}\quad\zeta\to 0, \tag{B7}$$

where

$$Ł=12\ln(2\sqrt{\pi})-7-8\pi^2\int_{-\delta}^{\infty}d\xi\,\mathrm{Ai}(\xi)^4-8\pi^2\int_{\delta}^{\infty}d\xi\left[\mathrm{Ai}(-\xi)^4-\frac{3}{8\pi^2\xi}\right]+3\ln\delta. \tag{B8}$$

Of course, Ł is independent of δ. The preceding equation reads

$$Ł=12\ln(2\sqrt{\pi})-7-8\pi^2\int_{0}^{\infty}d\xi\,\mathrm{Ai}(\xi)^4-8\pi^2\int_{0}^{\infty}d\xi\left[\mathrm{Ai}(-\xi)^4-\frac{3}{8\pi^2(1+\xi)}\right]. \tag{B9}$$

The analytical evaluation of Ł is performed in Appendix C. It is of some interest to recast Eq. (B9) in a form that is amenable to numerical computation. With

$$\begin{aligned}\mathrm{Ai}(-\xi)^4=&e^{-i2\pi/3}\mathrm{Ai}(\xi e^{i\pi/3})^4+e^{i2\pi/3}\mathrm{Ai}(\xi e^{-i\pi/3})^4+4e^{i2\pi/3}\mathrm{Ai}(\xi e^{i\pi/3})^3\mathrm{Ai}(\xi e^{-i\pi/3})\\&+4e^{-i2\pi/3}\mathrm{Ai}(\xi e^{-i\pi/3})^3\mathrm{Ai}(\xi e^{i\pi/3})+\tfrac{3}{8}[\mathrm{Ai}(-\xi)^2+\mathrm{Bi}(-\xi)^2]^2,\end{aligned} \tag{B10}$$

where use is made of the known identity[17]

$$\mathrm{Ai}(\xi e^{\pm i\pi/3})=\tfrac{1}{2}e^{\mp i\pi/3}[\mathrm{Ai}(-\xi)\pm i\,\mathrm{Bi}(-\xi)], \tag{B11}$$

Eq. (B9) becomes

$$Ł=12\ln(2\sqrt{\pi})-7-24\pi^2\int_{0}^{\infty}d\xi\,\mathrm{Ai}(\xi)^4-3\pi^2\int_{0}^{\infty}d\xi\left\{[\mathrm{Ai}(-\xi)^2+\mathrm{Bi}(-\xi)^2]^2-\frac{1}{\pi^2(1+\xi)}\right\}. \tag{B12}$$

Carrying out the calculations to higher orders in ζ suggests that $\overline{G}_{\mathrm{P}}(\zeta)$ admits a Laurent expansion at $\zeta=0$. Calculating the residue at this double pole gives

$$G_{\mathrm{P}}(x)\sim\frac{3}{4\pi^2}\frac{\ln x}{x}-\frac{Ł}{8\pi^2 x}\quad\text{as}\quad x\to\infty. \tag{B13}$$

2. Integral $G_{\mathrm{N}}(x)$

The Mellin transform of $G_{\mathrm{N}}(x)$ reads

$$\overline{G}_{\mathrm{N}}(\zeta)=\int_{-\infty}^{\infty}d\xi\,[\mathrm{Ai}(\xi)^2]^{2+\zeta}\int_{0}^{\infty}dt\,\frac{t^{-\zeta}}{(1+t)^2}=\frac{\pi\zeta}{\sin\pi\zeta}\int_{-\infty}^{\infty}d\xi[\mathrm{Ai}(\xi)^2]^{2+\zeta}. \tag{B14}$$

The original inversion path should lie inside the strip $0<\mathrm{Re}\,\zeta<1$. Note that $\overline{G}_{\mathrm{N}}(\zeta)$ has a simple pole at $\zeta=0$, in contradistinction to the double pole of $\overline{G}_{\mathrm{P}}(\zeta)$. From formula (B7),

$$\overline{G}_{\mathrm{N}}(\zeta)=\frac{3}{4\pi^2\zeta}+\mathrm{O}(1)\quad\text{as}\quad\zeta\to 0, \tag{B15}$$

which in turn leads to

$$G_{\mathrm{N}}(x) \sim \frac{3}{4\pi^2 x} \quad \text{as} \quad x \to \infty. \tag{B16}$$

APPENDIX C: ON THE FOURIER INTEGRALS OF Ai$(x)^n$, $n=1,2,3,4$

Let

$$w_n(x) = \mathrm{Ai}(x)^n, \quad n: \text{ positive integer.} \tag{C1}$$

Each $w_n(x)$ admits the integral representation

$$w_n(x) = \frac{1}{2\pi} \int_{\mathcal{C}_n} d\lambda e^{-i\lambda x} \overline{w}_n(\lambda), \tag{C2}$$

where $\mathcal{C}_n$ is an infinite contour with asymptotes that are subject to the usual convergence requirements as $\lambda \to \infty$. $\overline{w}_n(\lambda)$ is holomorphic in any finite part of the λ plane, except possibly at $\lambda = 0$, and obeys

$$\overline{w}_n^*(\lambda) = \overline{w}_n(-\lambda^*). \tag{C3}$$

In this Appendix, the task is to determine $\overline{w}_n(\lambda)$ and the integration path $\mathcal{C}_n$ for $n=1,2,3,4$. The constant Ł of Appendix B is subsequently computed through the limit $\overline{w}_4(\lambda \to 0^+)$.

1. Case $n=1$

The case $n=1$ is well-known yet instructive and needs to be revisited. The starting point is Airy's equation

$$\frac{d^2 w_1}{dx^2} - x w_1 = 0. \tag{C4}$$

Therefore, $\overline{w}_1(\lambda)$ has to satisfy

$$\frac{d\overline{w}_1}{d\lambda} + i\lambda^2 \overline{w}_1 = 0. \tag{C5}$$

It follows that

$$\overline{w}_1(\lambda) = C_1 e^{-i\lambda^3/3}, \tag{C6}$$

where C_1 is a constant yet to be determined. The right-hand side of Eq. (C2) for $n=1$ uncovers a linear combination of Ai(x) and Bi(x). The contour $\mathcal{C}_1$ is chosen to lie in the lower half of the λ plane with asymptotes in the sectors $\{\lambda: -\pi < \mathrm{Arg}\,\lambda < -2\pi/3\}$ and $\{\lambda: -\pi/3 < \mathrm{Arg}\,\lambda < 0\}$, and be described from left to right, as depicted in Fig. 14.

With the change of variable $\lambda = \sqrt{x} q$, where x is positive and large, $\mathcal{C}_1$ is deformed into the steepest descents path

$$\mathrm{Im}\, q = -\sqrt{1 + (\mathrm{Re}\, q)^2/3}, \tag{C7}$$

that passes through the saddle point at $q = -i$. An elementary calculation gives

$$w_1(x) = \frac{C_1}{2\pi} \sqrt{x} \int_{\mathcal{C}_1} dq e^{-ix^{3/2}(q + q^3/3)} \sim \frac{C_1}{2\sqrt{\pi}} x^{-1/4} e^{-(2/3)x^{3/2}} \quad \text{as} \quad x \to +\infty. \tag{C8}$$

A comparison with the known formula for the large-x behavior of Ai(x) furnishes[17]

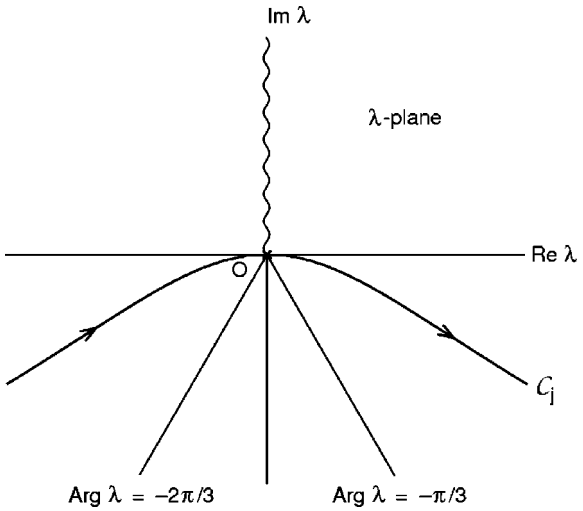

FIG. 14. Inversion path $\mathcal{C}_j$ $(j=1,2,3,4)$ for the Fourier transforms $\overline{w_j}(\lambda)$ of $\mathrm{Ai}(x)^j$ examined in Appendix C. The branch cut along the positive imaginary axis is necessary only for $j=2,3,4$.

$$C_1=1. \tag{C9}$$

The ensuing integral representation for $w_1(x)$ is

$$w_1(x)=\frac{1}{2\pi}\int_{\mathcal{C}_1} d\lambda\, e^{-i\lambda x-i\lambda^3/3}. \tag{C10}$$

2. Case $n=2$

$w_2(x)$ satisfies the third-order differential equation

$$\frac{d^3w_2}{dx^3}-4x\frac{dw_2}{dx}-2w_2=0, \tag{C11}$$

with solutions $\mathrm{Ai}(x)^2$, $\mathrm{Ai}(x)\mathrm{Bi}(x)$, and $\mathrm{Bi}(x)^2$. The Fourier transform of this equation is

$$4\lambda\frac{d\overline{w_2}}{d\lambda}+(i\lambda^3+2)\overline{w_2}=0, \tag{C12}$$

with the solution

$$\overline{w_2}(\lambda)=C_2\frac{e^{-i\lambda^3/12}}{\sqrt{\lambda}}. \tag{C13}$$

The first Riemann sheet is defined so that $\sqrt{\lambda}$ is positive for $\lambda>0$, with the branch cut lying in the upper half of the λ plane, as shown in Fig. 14. The integration path $\mathcal{C}_2$ is subsequently chosen as in the case with $n=1$. With the change of variable $\lambda=2\sqrt{x}q$, the leading saddle-point contribution at $q=-i$ is

$$w_2(x)=\frac{C_2}{\sqrt{2}\,\pi}x^{1/4}\int_{\mathcal{C}_2}\frac{dq}{\sqrt{q}}e^{-2ix^{3/2}(q+q^3/3)}=\frac{C_2}{2\sqrt{\pi}}e^{i\pi/4}x^{-1/2}e^{-(4/3)x^{3/2}} \quad \text{as } x\to+\infty. \tag{C14}$$

It follows that

$$C_2=\frac{e^{-i\pi/4}}{2\sqrt{\pi}}. \tag{C15}$$

$w_2(x)$ is

$$w_2(x)=\frac{e^{-i\pi/4}}{4\pi\sqrt{\pi}}\int_{\mathcal{C}_2} d\lambda\, e^{-i\lambda x}\frac{e^{-i\lambda^3/12}}{\sqrt{\lambda}}. \tag{C16}$$

Alternatively, one may have recourse to the convolution integral

$$\frac{1}{2\pi}\int_{\mathcal{C}_1} dt\, \overline{w}_1(t)\overline{w}_1(\lambda-t)=\frac{e^{-i\pi/4}}{2\sqrt{\pi\lambda}}e^{-i\lambda^3/12}. \tag{C17}$$

Clearly, the appropriate branch for the square root is selected via condition (C3).

3. Case $n=3$

In light of the foregoing analysis, it is straightforward yet somewhat laborious to calculate the Fourier transform of $\mathrm{Ai}(x)^3$. The starting point is the differential equation

$$\frac{d^4w_3}{dx^4}-10x\frac{d^2w_3}{dx^2}-10\frac{dw_3}{dx}+9x^2w_3=0, \tag{C18}$$

which has solutions $\mathrm{Ai}(x)^3$, $\mathrm{Ai}(x)^2\mathrm{Bi}(x)$, $\mathrm{Ai}(x)\mathrm{Bi}(x)^2$, and $\mathrm{Bi}(x)^3$, and is transformed into

$$9\frac{d^2\overline{w}_3}{d\lambda^2}+10i\lambda^2\frac{d\overline{w}_3}{d\lambda}-(\lambda^4-10i\lambda)\overline{w}_3=0. \tag{C19}$$

Let

$$\overline{w}_3(\lambda)=e^{-iu}Y(u),\quad u=\tfrac{5}{27}\lambda^3. \tag{C20}$$

Equation (C19) reads

$$u\frac{d^2Y}{du^2}+\frac{2}{3}\frac{dY}{du}+\frac{16}{25}uY=0. \tag{C21}$$

$Y(u)$ can be determined through the replacement

$$Y(u)=u^{\nu}Z_{\mu}(\beta u), \tag{C22}$$

where Z_μ denotes any Bessel function of order μ. Equation (C21) is satisfied if and only if

$$\mu=\pm\tfrac{1}{6},\quad \nu=\tfrac{1}{6},\quad \beta=\pm\tfrac{4}{5}. \tag{C23}$$

Accordingly, the general solution to Eq. (C19) is

$$\overline{w}_3(\lambda)=C_3\sqrt{\lambda}\left[J_{1/6}\left(\frac{4\lambda^3}{27}\right)+\tilde{C}_3H^{(2)}_{1/6}\left(\frac{4\lambda^3}{27}\right)\right]e^{-i5\lambda^3/27}. \tag{C24}$$

With the branch cut lying in the upper half of the λ plane so that $-2\pi+\theta_0<\mathrm{Arg}\,\lambda\leqslant\theta_0$, $0<\theta_0<\pi$, the integration path $\mathcal{C}_3$ is chosen as in the case with $n=2$ (see Fig. 14 for $\theta_0=\pi/2$). By virtue of the analytic continuation formulas[10]

$$J_{1/6}(e^{-i2\pi}z)=e^{-i\pi/3}J_{1/6}(z), \tag{C25}$$

$$H^{(2)}_{1/6}(e^{-i2\pi}z)=-H^{(2)}_{1/6}(z)-\sqrt{3}e^{i\pi/6}H^{(1)}_{1/6}(z), \tag{C26}$$

Eq. (C24) is equivalent to

$$\overline{w}_3(e^{-i\pi/2}\zeta)=C_3e^{-i\pi/4}\sqrt{\zeta}\left[\left(\frac{1}{2}e^{-i\pi/3}-\tilde{C}_3\sqrt{3}e^{i\pi/6}\right)H^{(1)}_{1/6}\left(i\frac{4\zeta^3}{27}\right)\right.$$
$$\left.+\left(\frac{1}{2}e^{-i\pi/3}-\tilde{C}_3\right)H^{(2)}_{1/6}\left(i\frac{4\zeta^3}{27}\right)\right]e^{5\zeta^3/27}. \tag{C27}$$

In the Fourier inversion formula, the saddle-point contribution stemming from the $H^{(2)}_{1/6}$ term is dominant unless

$$\tilde{C}_3=\tfrac{1}{2}e^{-i\pi/3}. \tag{C28}$$

The preceding value of $\tilde{C}_3$ ensures that the leading exponential for $w_3(x)$ as $x\to+\infty$ agrees with the known asymptotic formula for $\mathrm{Ai}(x)$.[17] In some detail, with Eq. (C28) and the large-argument approximation for $H^{(1)}_{1/6}(z)$,[10]

$$w_3(x)=\frac{C_3}{4\pi}e^{i\pi/4}\int_{\mathcal{C}_3'}d\zeta\,\sqrt{\zeta}H^{(1)}_{1/6}\left(i\frac{4\zeta^3}{27}\right)e^{5\zeta^3/27-\zeta x}\quad(\zeta=3\sqrt{x}t)$$
$$\sim\frac{C_3}{4\pi\sqrt{2\pi}}3^{3/2}e^{-i\pi/3}e^{-2x^{3/2}}\int_{1-i\infty}^{1+i\infty}dt\,e^{3x^{3/2}(t-1)^2}$$
$$=\frac{3C_3}{4\pi\sqrt{2}}e^{i\pi/6}x^{-3/4}e^{-2x^{3/2}}\quad\text{as}\quad x\to\infty, \tag{C29}$$

where $\mathcal{C}_3'$ results from the counterclockwise rotation of $\mathcal{C}_3$ by $\pi/2$ about the origin. Hence,

$$C_3=\frac{e^{-i\pi/6}}{3\sqrt{2\pi}}. \tag{C30}$$

The desired Fourier representation for $w_3(x)$ is

$$w_3(x)=\frac{e^{-i\pi/6}}{6\pi\sqrt{2\pi}}\int_{\mathcal{C}_3}d\lambda\,e^{-i\lambda x}\sqrt{\lambda}\left[J_{1/6}\left(\frac{4\lambda^3}{27}\right)+\frac{1}{2}e^{-i\pi/3}H^{(2)}_{1/6}\left(\frac{4\lambda^3}{27}\right)\right]e^{-i5\lambda^3/27}. \tag{C31}$$

4. Case $n=4$

The differential equation

$$\frac{d^5w_4}{dx^5}-20x\frac{d^3w_4}{dx^3}-30\frac{d^2w_4}{dx^2}+64x^2\frac{dw_4}{dx}+64xw_4=0, \tag{C32}$$

with solutions $\mathrm{Ai}(x)^4$, $\mathrm{Ai}(x)^3\mathrm{Bi}(x)$, $\mathrm{Ai}(x)^2\mathrm{Bi}(x)^2$, $\mathrm{Ai}(x)\mathrm{Bi}(x)^3$, and $\mathrm{Bi}(x)^4$, is transformed into

$$64i\lambda\frac{d^2\overline{w}_4}{d\lambda^2}-(20\lambda^3-64i)\frac{d\overline{w}_4}{d\lambda}-(i\lambda^5+30\lambda^2)\overline{w}_4=0. \tag{C33}$$

Evidently, this equation can be solved via the substitutions

$$\overline{w}_4(\lambda)=e^{-iu}Z_0(3u/5),\quad u=\tfrac{5}{96}\lambda^3. \tag{C34}$$

Z_0 is any Bessel function of order 0. The general solution to Eq. (C33) reads

$$\overline{w}_4(\lambda)=C_4\left[J_0\left(\frac{\lambda^3}{32}\right)+\tilde{C}_4H_0^{(2)}\left(\frac{\lambda^3}{32}\right)\right]e^{-i5\lambda^3/96}. \tag{C35}$$

The first Riemann sheet and the integration path $\mathcal{C}_4$ are chosen as in Appendix C 3 (see Fig. 14). Consider the analytic continuation formula

$$\overline{w}_4(e^{-i\pi/2}\zeta)=C_4\left[\left(\frac{1}{2}-2\tilde{C}_4\right)H_0^{(1)}\left(i\frac{\zeta^3}{32}\right)+\left(\frac{1}{2}-\tilde{C}_4\right)H_0^{(2)}\left(i\frac{\zeta^3}{32}\right)\right]e^{5\zeta^3/96}. \tag{C36}$$

The coefficient $\tilde{C}_4$ is determined by elimination of the $H_0^{(2)}$ term in this equation:

$$\tilde{C}_4=\tfrac{1}{2}. \tag{C37}$$

A standard steepest-descent calculation as in Eq. (C29) then gives

$$w_4(x)=-\frac{C_4}{4\pi}e^{-i\pi/2}\int_{\mathcal{C}_4'}d\zeta\,H_0^{(1)}\left(i\frac{\zeta^3}{32}\right)e^{5\zeta^3/96-\zeta x}$$

$$\sim i\frac{C_4}{2\pi x}e^{-(8/3)x^{3/2}}\quad\text{as}\quad x\to+\infty. \tag{C38}$$

Comparison with the leading term for $\mathrm{Ai}(x)^4$ from Ref. 17 yields

$$C_4=-\frac{i}{8\pi}. \tag{C39}$$

Consequently,

$$w_4(x)=\frac{1}{16\pi^2 i}\int_{\mathcal{C}_4}d\lambda\,e^{-i\lambda x}\left[J_0\left(\frac{\lambda^3}{32}\right)+\frac{1}{2}H_0^{(2)}\left(\frac{\lambda^3}{32}\right)\right]e^{-i5\lambda^3/96}. \tag{C40}$$

Alternatively, one may employ the convolution integral

$$\overline{w}_4(\lambda)=\frac{1}{2\pi}\int_{-\infty}^{+\infty}dt\,\overline{w}_2(\lambda-t)\overline{w}_2(t)\quad[t=\lambda(\tau+1)/2]$$

$$=\frac{e^{-i\lambda^3/48}}{4\pi^2}\left(-i\int_0^1 d\tau\frac{e^{-i\lambda^3\tau^2/16}}{\sqrt{1-\tau^2}}+\int_1^\infty d\tau\frac{e^{-i\lambda^3\tau^2/16}}{\sqrt{\tau^2-1}}\right)$$

$$=\frac{e^{-i5\lambda^3/96}}{8\pi^2}\left(-i\int_0^\pi d\theta\,e^{i\lambda^3\cos\theta/32}+\int_0^\infty d\theta\,e^{-i\lambda^3\cosh\theta/32}\right), \tag{C41}$$

which immediately leads to Eq. (C40). In the above, the changes of variable $\tau=\sin(\theta/2)$ and $\tau=\cosh(\theta/2)$ are made in the first and second integral of the second line, respectively.

5. Analytical evaluation of Ł

On the basis of Eq. (C40), it is a simple task to calculate explicitly the Ł of Eq. (B9) of Appendix B. This equation is recast in the form

$$Ł = 12\ln(2\sqrt{\pi}) - 7 - 8\pi^2 \lim_{\lambda\to 0^+} \int_{-\infty}^{+\infty} dx\, e^{i\lambda x}[\mathrm{Ai}(x)^4 - b(x)], \tag{C42}$$

where

$$b(x) = \begin{cases} \dfrac{3}{8\pi^2}\dfrac{1}{1-x}, & x<0 \\ 0, & x>0. \end{cases} \tag{C43}$$

Note that the function $\mathrm{Ai}(x)^4 - b(x)$ is absolutely integrable, while each one of $\mathrm{Ai}(x)^4$ and $b(x)$ is square integrable in $(-\infty,\infty)$. For the sake of some routine rigor, it is advisable to invoke the Fourier–Plancherel operator[23] and rewrite Eq. (C42) as

$$Ł = 12\ln(2\sqrt{\pi}) - 7 - 8\pi^2 \lim_{\lambda\to 0^+} \frac{d}{d\lambda}\left[\int_{-\infty}^{\infty} dx \frac{e^{i\lambda x}-1}{ix}\mathrm{Ai}(x)^4 - \int_{-\infty}^{\infty} dx \frac{e^{i\lambda x}-1}{ix} b(x)\right]. \tag{C44}$$

The second integral is calculated explicitly to give

$$\frac{d}{d\lambda}\int_{-\infty}^{\infty} dx \frac{e^{i\lambda x}-1}{ix} b(x) = -\frac{3}{8\pi^2} e^{i\lambda}\,\mathrm{Ei}(-i\lambda)$$

$$\sim -\frac{3}{8\pi^2}\left(\ln\lambda + \gamma + \frac{i\pi}{2}\right) \quad \text{as } \lambda\to 0^+, \tag{C45}$$

where $\mathrm{Ei}(-z)$ is the exponential integral.[16] The integral involving $\mathrm{Ai}(x)^4$ follows from Plancherel's theorem[23,24] and Eq. (C40), along with the approximations

$$J_0(z)\sim 1, \quad H_0^{(2)}(z)\sim 1 - \frac{2i}{\pi}\left(\gamma + \ln\frac{z}{2}\right) \quad \text{as } z\to 0. \tag{C46}$$

Accordingly,

$$\frac{d}{d\lambda}\int_{-\infty}^{\infty} dx \frac{e^{i\lambda x}-1}{ix}\mathrm{Ai}(x)^4 = \overline{w}_4(\lambda)$$

$$\sim \frac{3}{16\pi i} - \frac{3\ln\lambda + \gamma - 6\ln 2}{8\pi^2} \quad \text{as } \lambda\to 0^+. \tag{C47}$$

The combination of Eqs. (C44), (C45), and (C47) furnishes

$$Ł = 6\ln(2\pi) - 2\gamma - 7. \tag{C48}$$

This result agrees with the numerical calculation based on Eq. (B12) of Appendix B.

[1] D. Margetis, G. Fikioris, J. M. Myers, and T. T. Wu, Phys. Rev. E **58**, 2531 (1998).
[2] B. Z. Katsenelenbaum and M. Yu. Shalukhin, Radiotekh. Elektron. (Moscow) **33**, 1878 (1988) [Sov. J. Commun. Technol. Electron. **34**, 25 (1989)].
[3] T. S. Angell and A. Kirsch, Math. Methods Appl. Sci. **15**, 647 (1992); T. S. Angell, R. E. Kleinman, and B. Vainberg, SIAM (Soc. Ind. Appl. Math.) J. Appl. Math. **59**, 242 (1998).
[4] G. Fikioris, Ph.D. thesis, Harvard University, 1993.
[5] G. Fikioris, J. Electromagn. Waves Appl. **10**, 307 (1996).
[6] Various issues of routine rigor such as the interpretation of the Laplacian, the nature of the limit at the boundary, and the admissible data $h(s)$ are not addressed in this paper. It is sufficient although not necessary to state that $\mathcal{C}$ is a simple closed, rectifiable, and infinitely differentiable curve.
[7] The exterior R^e of $\mathcal{C}$ mentioned here is the set $\mathcal{E}_2\backslash R$. Of course, in the limiting process that is implied by the fourth line of Eq. (2.1), $\mathbf{r}$ belongs to R^e without lying in $\mathcal{C}$.

[8] F. G. Tricomi, *Integral Equations* (Dover, New York, 1985). For present purposes, the definition of the Fredholm integral equation of the second kind is the one where the integral $\int_C \int_C d\mathbf{r}\, d\mathbf{r}'\, |K(\mathbf{r},\mathbf{r}')|^2$ is assumed to exist and be finite.
[9] A finite-dimensional version of the present problem involves the maximization of a linear function over the intersection of a sphere and an ellipsoid. Accordingly, no complication of any kind should arise in the use of the Lagrange multipliers.
[10] Bateman Manuscript Project, *Higher Transcendental Functions*, edited by A. Erdélyi (Krieger, Malabar, FL, 1981), Vol. II, pp. 80, 81, 85, 86, 87, 96, 102, 317.
[11] For the statement of a theorem underlying the Poisson summation formula see T. M. Apostol, *Mathematical Analysis* (Addison–Wesley, Reading, MA, 1974), pp. 332–335.
[12] O. I. Marichev, *Integral Transforms of Higher Transcendental Functions* (Horwood, Chichester, 1983).
[13] R. J. Sasiela and J. D. Shelton, J. Math. Phys. **34**, 2572 (1993).
[14] Of course, the logarithmic derivative $\psi(z)$ of the gamma function here should not be confused with the $\psi(\hat{\mathbf{r}})$ of Eq. (2.4).
[15] B. J. Stoyanov and R. A. Farrell, Math. Comput. **49**, 275 (1987). These authors calculate only the first three terms of the asymptotic expansion (3.30). Their method does not make use of the Mellin transform technique.
[16] Bateman Manuscript Project, *Higher Transcendental Functions*, edited by A. Erdélyi (Krieger, Malabar, FL, 1981), Vol, I, pp. 101, 182, 267.
[17] *Handbook of Mathematical Functions*, edited by M. Abramowitz and I. A. Stegun (Dover, New York, 1972), pp. 365–367, 446.
[18] D. Margetis, Chap. 5 of Ph.D. thesis, Harvard University, 1999.
[19] C. W. Oseen, Ann. Phys. (Leipzig) **69**, 202 (1922).
[20] The failure of expression (8.27) in the vicinity of $\phi=0$ is suggested by the nonphysical result that the limits $\lim_{\alpha\to 0}\lim_{\phi\to 0}$ and $\lim_{\phi\to 0}\lim_{\alpha\to 0}$ of its right-hand side are not equal.
[21] For a fixed point in C and a fixed number of reflections, the contributing rays can result from minimizing the total length of all possible paths that originate from a line of reference, by running parallel or antiparallel to the direction of maximum field.
[22] G. N. Watson, Proc. R. Soc. London, Ser. A **95**, 83 (1918).
[23] N. I. Akhiezer and I. M. Glazman, *Theory of Linear Operators in Hilbert Space* (Dover, New York, 1993), Vol. I, pp. 74–77.
[24] E. C. Titchmarsh, *Introduction to the Theory of Fourier Integrals* (Chelsea, New York, 1986), p. 69.